AD-A088 856 UTAH UNIV SALT LAKE CITY DEPT OF MATERIALS SCIENCE --ETC F/G 11/6
POSITRON ANNIHILATION GAMMA RAY LINESHAPE STUDIES OF DEFECTS IN--ETC(U)
JUN 80 J G BYRNE AFOSR-75-2810
UNCLASSIFIED UTEC-80-092 AFOSR-TR-80-0700 NL

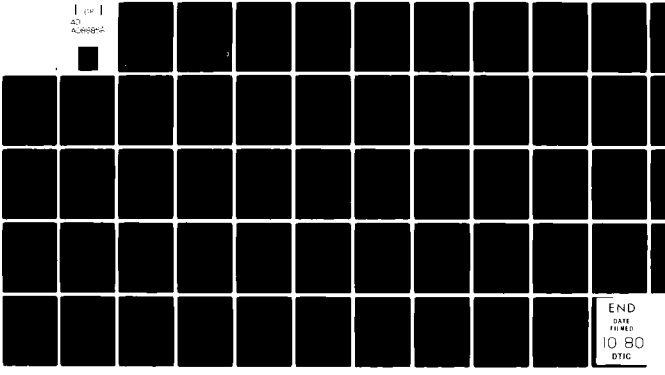

END
DATE FILMED
10-80
DTIC

Unclassified

SECURITY CLASSIFICATION OF THIS PAGE (When Data Entered) LEVEL II

12

19 REPORT DOCUMENTATION PAGE

READ INSTRUCTIONS BEFORE COMPLETING FORM

1. REPORT NUMBER: AFOSR-TR-80-0700
2. GOVT ACCESSION NO.: AD-A088856
3. RECIPIENT'S CATALOG NUMBER:

4. TITLE (and Subtitle): POSITRON ANNIHILATION GAMMA RAY LINESHAPE STUDIES OF DEFECTS IN SOLIDS
5. TYPE OF REPORT & PERIOD COVERED: Final: 1 April 1975 to 31 March 1980
6. PERFORMING ORG. REPORT NUMBER:

7. AUTHOR(s): DR. J. G. BYRNE
8. CONTRACT OR GRANT NUMBER(s): AFOSR-75-2810

9. PERFORMING ORGANIZATION NAME AND ADDRESS:
Department of Materials Science & Engineering
University of Utah
Salt Lake City, Utah 84112

10. PROGRAM ELEMENT, PROJECT, TASK AREA & WORK UNIT NUMBERS: 61102F 2306/A2

11. CONTROLLING OFFICE NAME AND ADDRESS:
AFOSR/NE
Bldg. 410, Bolling AFB
Washington D. C. 20332

12. REPORT DATE: June 1980
13. NUMBER OF PAGES: 64

14. MONITORING AGENCY NAME & ADDRESS (if different from Controlling Office): Final rept. 1 Apr 75-31 Mar 80

15. SECURITY CLASS. (of this report): Unclassified
15a. DECLASSIFICATION/DOWNGRADING SCHEDULE: N.A.

16. DISTRIBUTION STATEMENT (of this Report)

Approved for public release; distribution unlimited.

17. DISTRIBUTION STATEMENT (of the abstract entered in Block 20, if different from Report)

DTIC ELECTE SEP 4 1980 S D

18. SUPPLEMENTARY NOTES

19. KEY WORDS (Continue on reverse side if necessary and identify by block number)
positron annihilation, Doppler broadening, precipitation, defects in solids, dislocations, precipatate interfaces, phase interfaces, non-destructive evaluation of hydrogen embrittlement, hydrogen embrittlement

20. ABSTRACT (Continue on reverse side if necessary and identify by block number)
Positron annihilation measurements, performed via Doppler broadening of the annihilation gamma photon energy distributions, have been effectively applied to follow age hardening, hydrogen embrittlement, dislocation generation during single crystal bending, phase transformations in steel, deformation of both samples containing precipitates and pre-precipitates and the deformation of steel. The technique is non-destructive and sensitive to line and point defects, interfaces and microvoids.

DD FORM 1 JAN 73 1473 EDITION OF 1 NOV 65 IS OBSOLETE

Unclassified

SECURITY CLASSIFICATION OF THIS PAGE (When Data Entered)

AD A088856

DDC FILE COPY

80 9 2 056

AFOSR-TR- 80-0700

UTEC 80-092

FINAL REPORT TO THE

AIR FORCE OFFICE OF SCIENTIFIC RESEARCH

ON GRANT AFOSR-75-2810J

TERMINATION DATE MARCH 31, 1980

# POSITRON ANNIHILATION GAMMA RAY LINESHAPE STUDIES OF DEFECTS IN SOLIDS

by

Dr. J. G. Byrne

Department of Materials Science and Engineering

University of Utah

Salt Lake City, Utah 84112



June, 1980

TABLE OF CONTENTS

## ABSTRACT

Positron annihilation measurements, performed via Doppler broadening of the annihilation gamma photon energy distributions, have been effectively applied to follow age hardening, hydrogen embrittlement, dislocation generation during single crystal bending, phase transformations in steel, deformation of both samples containing precipitates and pre-precipitates and the deformation of steel. The technique is nondestructive and sensitive to line and point defects, interfaces, and microvoids.

# 1. INTRODUCTION

This final report first summarizes the work accomplished prior to the Preliminary Report of September, 1979, and then describes in detail the results obtained from that time to March 31, 1980.

## Summary of Work Prior to September, 1979

1. The Trapping of Positrons by Dislocations Produced in Single Crystal Bending, M. L. Johnson, S. Saterlie and J. G. Byrne, Met. Trans. 9A (1978) 841. (copy attached)

This work established the trapping efficiency of edge dislocations for positrons and we think will prove to be a key contribution in a controversial area.

2. The Removal of Defects from Solids as Observed with Positron Annihilation, M. L. Johnson, S. Saterlie, D. Boice and J. G. Byrne, Phys. Stat. Solidi (a), 48 (1978) 83. (copy attached)

This work showed the comparison of annealing effects measured with positron parameters and with hardness.

3. Positron Measurements of Aging in Complex Al Alloys, M. L. Johnson, S. Panchanadeeswaran, S. Saterlie, and J. G. Byrne, Phys. Stat. Solidi, 42 (1977) 175. (copy attached)

4. Positron Trapping at Precipitates in Al-4 wt% Cu Single Crystals, S. Panchanadeeswaran, R. W. Ure and J. G. Byrne, Phys. Stat. Solidi, 48 (1978) 83. (copy attached).

5. Positron Annihilation Observations of Shot Peened Al Alloys, S. Saterlie, M. L. Johnson, P. Alexopoulos, F. Seppi, R. Ure and J. G. Byrne, Phys. Stat. Solidi (a), 42 (1977) 175. (copy attached)

The above three works began to address the problems of positron interactions with precipitates.

6. A Study of Hydrogen Charging of Ni by Positron Doppler Broadening, P. W. Kao, R. W. Ure and J. G. Byrne, Phil. Mag., 39 (1979) 514 (copy attached).

This work showed the important fact that hydrogen embrittlement is detectable nondestructively with positron annihilation.

## Work Since September, 1979

Earlier, we reported[1] that aging a commercial aluminum base alloy, 7075, caused the Doppler peak to wings (P/W) shape measurements to respond to a maximum hardness aged condition in a similar way as to cold work in a pure metal. That is, the Doppler peak sharpens, or higher P/W values are found, because (in the cold worked state) more positrons are trapped and annihilate at dislocations where the population of higher energy core electrons is less.

To better understand the response of positrons to aging, we produced well-known conditions involving Guinier-Preston zones, pre-precipitates, transition precipitates and equilibrium precipitates in both single and polycrystalline Al-4wt% Cu specimens and measured the P/W parameter as a function of depth[2] using positrons of differing penetration depths.

### 2. Aluminum Alloy Single Crystals

#### 2.1 Aging Effects

These effects are contained in references (2) and (6) which are attached and show that the P/W parameter rose from its level for a solid solution to a maximum for the GP zone conditions then declined as θ' and θ occurred during aging. It appears that the strains around GP zones are much more interactive with positrons than are either the point defect distribution created by quenching or the interface of θ' and θ particles with the matrix.

## 2.2 Deformation Following Aging

More recently single crystals containing the carefully characterized aged states mentioned in section 2.1 were deformed in tension while Doppler measurements were made. The purpose was to ascertain how the various well-known particle-dislocation interactions[3] would respond to positrons. For example, GPI zones are cut by dislocations as are GPII zones, however, only in the second case, is internal disorder created in the particles by the cutting. There was essentially no response of positrons to the cutting of GPI as is seen by $I_V$ (the ratio of peak counts to total counts) in Fig. 3 of reference (6). $I_V$ also does not change with straining for the dislocation cutting of GPII zones (Fig. 4, of reference (6) ) even where internal disorder is created. This is quite different for the $I_V$ change with strain for the deformation of θ' and θ containing single crystals as seen in Figs. 5 and 6 of reference (6), respectively. The increase in $I_V$ is larger and faster for the surrounding of θ' particles with dislocation loops than for the same event involving θ particles. N.B. reference (6) is attached.

# 3. Aluminum Alloy Polycrystals

## 3.1 Aging Effects

In order to examine an aging system which passes from a condition involving complete coherency with lesser coherency strains than in the Al-Cu alloy case, samples of an Al-10wt% Zn alloy were studied. Very recent results, not yet submitted for publication, will now be described.

Samples were quenched from a solution treatment temperature of 350°C and aged cumulatively for six hours at each of six temperatures ranging from 25°C to 220°C. The P/W parameter increased parabolically with increasing aging time, however, it may be more instructive for us to

consider the $I_V$ (Peak/Total) and $I_C$ (Wings/Total) parameters since they delineate the peak and wing regions behaviors more clearly. Fig. 1 shows that the $I_V$ parameter rose 2.2% for aging up to about 100°C and then flattened up to 22°C. The $I_C$ parameter decreased steadily over the whole range. It would seem then, from the $I_V$ data, that positron trapping in the coherency strain field of the early aged states saturates between 80 and 130°C, while the parameter $I_C$, reflective of the higher core electron wing region response of zinc, responds all the way from the lowest to the highest aging temperature. The latter response suggests that the homogenous distribution of zinc atoms in the initial solid solution makes the zinc more apparent to the positrons than later in the aging process when the solid solution has been depleted to for $\alpha'$ and later equilibrium precipitates. This latter tendency (seen only with $I_V$) of trapping and annihilating with higher energy core electrons of zind atoms (rather than aluminum atoms) seems more important than the coherency strain field trapping seen with $I_V$, because the latter soon saturates out but the former tendency persists throughout the aging temperature range thus far studied. Figure 2 further exemplified this fact with $Al^+$ 8.5 w/o Zn polycrystalline samples quenched from 550°C and aged at temperatures of 68, 84, 100 and 115°C. One can see in Fig. 2b that the depletion of Zn atoms from the solid solution during aging, for example at 115°C, is felt twice as much by $I_C$ (Wings/Total) as by $I_V$ (Peak/Total) in Fig. 2a.

## 4. Measurements in Steels

### 4.1 Effects Due to % C in Plain Carbon Steels

The increase in the amount of pearlite in normalized plain carbon steels as the carbon content increases is seen in Fig. 3.

Some additional results with these samples are that 70% cold rolling of the 1020 steel increases P/W to 2.705.

In 1080 steel if one, by different isothermal transformation temperatures, produces first coarse then fine pearlite, typical P/W values for those two structures are 2.347 and 2.425 respectively.

Some fatigue effects were detected in 1020 steel which had been given heavy cold rolling plus an intercritical anneal and a brine quench to produce oriented martensite in a matrix of ferrite. These P/W values increased with the number of cycles at a maximum alternating stress of 88 psi (606.7 MPa) but not in a steady way. Fig. 3 shows a plateau at P/W = 2.35 up to 5 X $10^3$ cycles, a slight rise from 2.35 to 2.39 at 10 X $10^3$ cycles where slip bands could be seen forming on the surface, then an abrupt increase to 2.43 - 2.45 where it held to 20 X $10^3$ cycles, then a final increase to 2.50 by fracture at 30 X $10^3$ cycles.

4.2 Effects Due to Changes in Surface to Volume Ratio of $Fe_3C$

Fig. 5 shows how the P/W (denoted as P in this figure) rises as the cementite surface to volume ratio increases. This suggests that interface trapping is involved. The same conclusion is consistent with the decrease in P/W with increasing spacing between cementite particles.

4.3 R Parameter and Trapping Mechanisms

The R parameter[4] is designed to detect a change of mechanism during positron measurements of a sequence of events. It is defined as:

$$R = \left| \frac{I_v - I_v^f}{I_c - I_c^f} \right|$$

where $I_v$ and $I_c$, as defined earlier, are the ratios of peak to total and wings to total counts respectively. $I_v^f$ and $I_c^f$ are similar quantities

except in a reference sample where most of the positrons annihilate in perfect material or a "free" (f) state.

R was calculated for various normalized steels and for one of them (1010) in a cold rolled condition. The results are as follows:

| Steel | Condition | R Value |
|---|---|---|
| 1010 | Normalized | 1.549 |
| 1020 | Normalized | 1.562 |
| 1060 | Normalized | 1.542 |
| 1080 | Normalized | 1.555 |
| 1020 | Cold-rolled | 1.659 |

The sharp increase in R for the cold-rolled 1020 steel signals that a change in trapping mechanism occurred, i.e. positrons in the cold-rolled sample probably are trapping at dislocations rather than at the ferrite-cementite interfaces.

4.4 Other Positron Studies in Steel

Interlamellar spacings, microhardness and x-ray particle sizes and microstrains were measured along with the P/W Doppler parameter for eutectoid steel after a series of heat treatments designed to gradually change the interlamellar spacing. Dislocation densities were calculated as shown by Williamson and Smallman[5] from the x-ray particle sizes. The heat treatments were as follows:

| Heat Treatment No. | Isothermal T (°C) | Time (sec) |
|---|---|---|
| 1 | 600 | 120 |
| 2 | 630 | 240 |

| Heat Treatment No. | Isothermal T (°C) | Time (sec) |
|---|---|---|
| 3 | 660 | 360 |
| 4 | 675 | 1200 |
| 5 | 690 | 1800 |

The interlamellar spacing, microhardness, P/W value and average x-ray particle size, $\overline{D}$, for the various treatments are:

| Heat Treatment | Interlamellar Spacing, S | Microhardness Hv (200 g load) | P/W | $\overline{D}$ (Å) |
|---|---|---|---|---|
| 1 | 1125 | 334 | 2.8436 | 1012 |
| 2 | 1260 | 302 | --- | --- |
| 3 | 1326 | 288 | 2.776 | 1195 |
| 4 | 1690 | 240 | 2.727 | 1472 |
| 5 | 2200 | 208 | 2.690 | 1164 |
| As Rolled | --- | --- | 3.3842 | 716 |

The P/W values increase quite linearly with increasing values of $S^{-1}$ and also with increasing values of microhardness, Hv. If one plots the calculated dislocation density from the x-ray data against P/W value, linearity is found for the four heat treatments (1, 3, 4 and 5) but the point for the cold-rolled condition falls far below the extrapolation for the isothermal heat treatments. This appears to be another evidence that the different R parameter values, discussed in section 4.3, were indicating a different trapping mechanism for the cold-worked state compared with the various annealed conditions.

The fractional concentration of dislocation cores, C, is defined as the number of dislocations emerging on a surface per $cm^2$ divided by the

number of atoms on that surface per $cm^2$ and is given by

$$C_D = \frac{\lambda_f}{\mu} \cdot \frac{(P/W) - (P/W)_f}{(P/W)_t - (P/W)}$$

where $C_D = \rho/d$, d is the number of atoms per $cm^2$ and $\rho$ is the dislocation density in $cm^{-2}$,

$\mu$: positron trapping rate, and

$\lambda_f$: the annihilation rate of untrapped positrons in the material.

$(P/W)_f$ and $(P/W)_t$ are the peak to wings ratio of a fully annealed sample and of a highly deformed sample, respectively. In the case of low dislocation density, $(P/W) \simeq (P/W)_f$, then

$$C_D = \rho/d \simeq \frac{\lambda_f}{\mu \left[(P/W)_t - (P/W)_f\right]} \left[(P/W) - (P/W)_f\right]$$

or

$$(P/W) \simeq (P/W)_f + \left\{\frac{\mu \left[(P/W)_t - (P/W)_f\right]}{\lambda_f d}\right\} \rho .$$

We thus have a dilemma in that the P/W shape factor depends linearly on each of phase interfacial area per volume and dislocation density. The problem is to separate phase interface and dislocation contributions. We begin the solution of this problem by rewriting the last equation as follows:

$$(P/W) = (P/W)_f + \frac{\left[(P/W)_t - (P/W)_f\right]}{\lambda_f} \left[\mu_I C_I + \mu_D C_D\right]$$

where $\mu_I$ and $\mu_D$ are the positron trapping rates at phase interfaces and dislocations respectively. $C_I$, the fractional interface concentration requires definition. $C_I$ is obtained by dividing the interfacial surface area per volume, $A_c$ $(cm^{-1})$, by the number of atoms per cm in direct analogy

to the calculation of $C_D$ which is obtained by dividing the dislocation density ($cm^{-2}$) by d, the number of atoms per $cm^2$. The value of d for Fe is about $1.9 \times 10^{15}$ $cm^{-2}$. Thus the fractional interface concentration $C_I$, for any given pair of values of P/W and carbide area per volume, $A_c$, is caluclated by dividing $A_c$ by the number of atoms per cm, which for Fe is about $4.4 \times 10^7$ $cm^{-1}$.

Once having the values of $C_I$ and $C_D$ for each value of P/W and using the $\lambda_f$ value of $6.41 \times 10^9$ $sec^{-1}$ (see introduction) a linear regression analysis was used to obtain the trapping rates:

$$\mu_I = (5 \pm 2) \times 10^{10}\ s^{-1},$$

$$\mu_D = (2.1 \pm 0.1) \times 10^{14}\ s^{-1}\ .$$

The table below lists the values of $C_D$ and $C_I$ for each P/W value and in addition the relative probablities of trapping at phase interfaces,

$$P_I = \frac{\mu_I C_I}{\left[\lambda_f + \mu_I C_I + \mu_D C_D\right]}\ ,$$

and at dislocations,

$$P_D = \frac{\mu_D C_D}{\left[\lambda_f + \mu_I C_I + \mu_D C_D\right]}\ .$$

Consideration of the table below shows that, first of all, the sum of the probabilities for a given P/W is less than 100%. This is because these materials were all isothermally transformed, i.e. they were relatively soft and should cold work be added, $P_D$ should increase as the dislocation density increases. Secondly and of major interest here, the probability, $P_D$, of dislocations acting as traps is always at least an order of magnitude larger than $P_I$, the probability of interface trapping.

| P/W | $C_I$ | $C_D$ | $P_I$ (%) | $P_D$ (%) |
|---|---|---|---|---|
| 2.844 | $4.1 \times 10^{-3}$ | $10.2 \times 10^{-6}$ | 2.2 | 23.7 |
| 2.776 | $3.4 \times 10^{-3}$ | $8.2 \times 10^{-6}$ | 2.0 | 20.0 |
| 2.727 | $2.7 \times 10^{-3}$ | $5.8 \times 10^{-6}$ | 1.6 | 15.1 |
| 2.690 | $2.1 \times 10^{-3}$ | $5.0 \times 10^{-6}$ | 1.3 | 13.4 |

## 5. Hydrogen Embrittlement

These very interesting developments are fully described in reference (7) which is attached.

## 6. Si Studies

Considerable effort went into positron lifetime measurements of both n type and p type Si and of Si single crystal four-point bending at high temperatures, however, in no case were significant changes in positron parameters detected.

## 7. Other Activities Related to Grant

Some requested review articles are listed below which, although they do not report new results, do indicate outside interest and were made possible largely through the AFOSR research support.

1. Invitation from Dr. John P. Hirth to contribute a mini-review to Scripta Metallurgica's Annual Viewpoint Set. The Utility of Positrons for Studies of Metals and Alloys, Scripta Met., 14, (1980) 3. (copy attached)
2. AIME Symposium on Recovery, Recrystallization and Grain Growth, Met. Trans. A, 10 (1979) 791. (copy attached)
3. Invitation of Dr. F. R. N. Nabarro to contribute a chapter on dislocations and positrons for his forthcoming multi-volume solid state physics set on dislocations in solids, submitted 1980.

## 8. References


1. M. L. Johnson, S. Panchanadeeswaran, S. Saterlie, and J. G. Byrne, Phys. Stat. Sol. (a), 42, 175 (1977).

2. S. Panchanadeeswaran, R. W. Ure, Jr., and J. G. Byrne, Phys. Stat. Sol. (a), 48, 83 (1978).

3. J. G. Byrne, M. E. Fine and A. Kelly, Phil. Mag., 6, 1119 (1961).

4. S. Mantl and W. Triftshauser, Phys. Rev. Lett., 34, 1554 (1975).

5. G. K. Williamson and R. E. Smallman, Phil. Mag., 1, 34 (1956).

6. S. Panchanadeeswaran, Po-We Kao, R.W. Ure Jr., and J.G. Byrne, ARPA/AF Review of Progress in Quantitative NDE, 1979.

7. Po-We Kao, R.W. Ure, Jr., and J.G. Byrne, Phil. Mag. A39, 517 (1979).

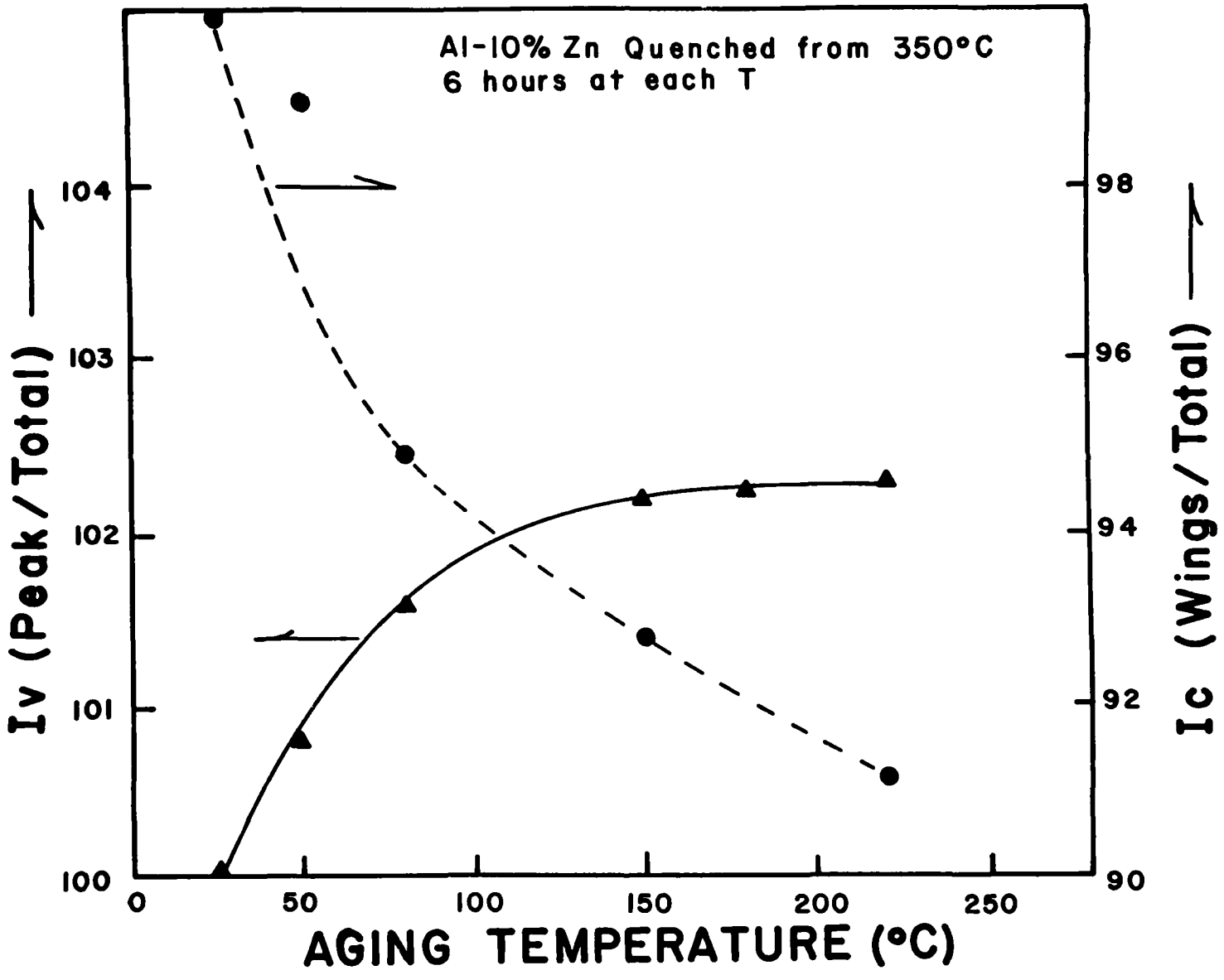
Al-10% Zn Quenched from 350°C
6 hours at each T
Iv (Peak/Total)
Ic (Wings/Total)
104
103
102
101
100
98
96
94
92
90
0
50
100
150
200
250
AGING TEMPERATURE (°C)

Figure 1

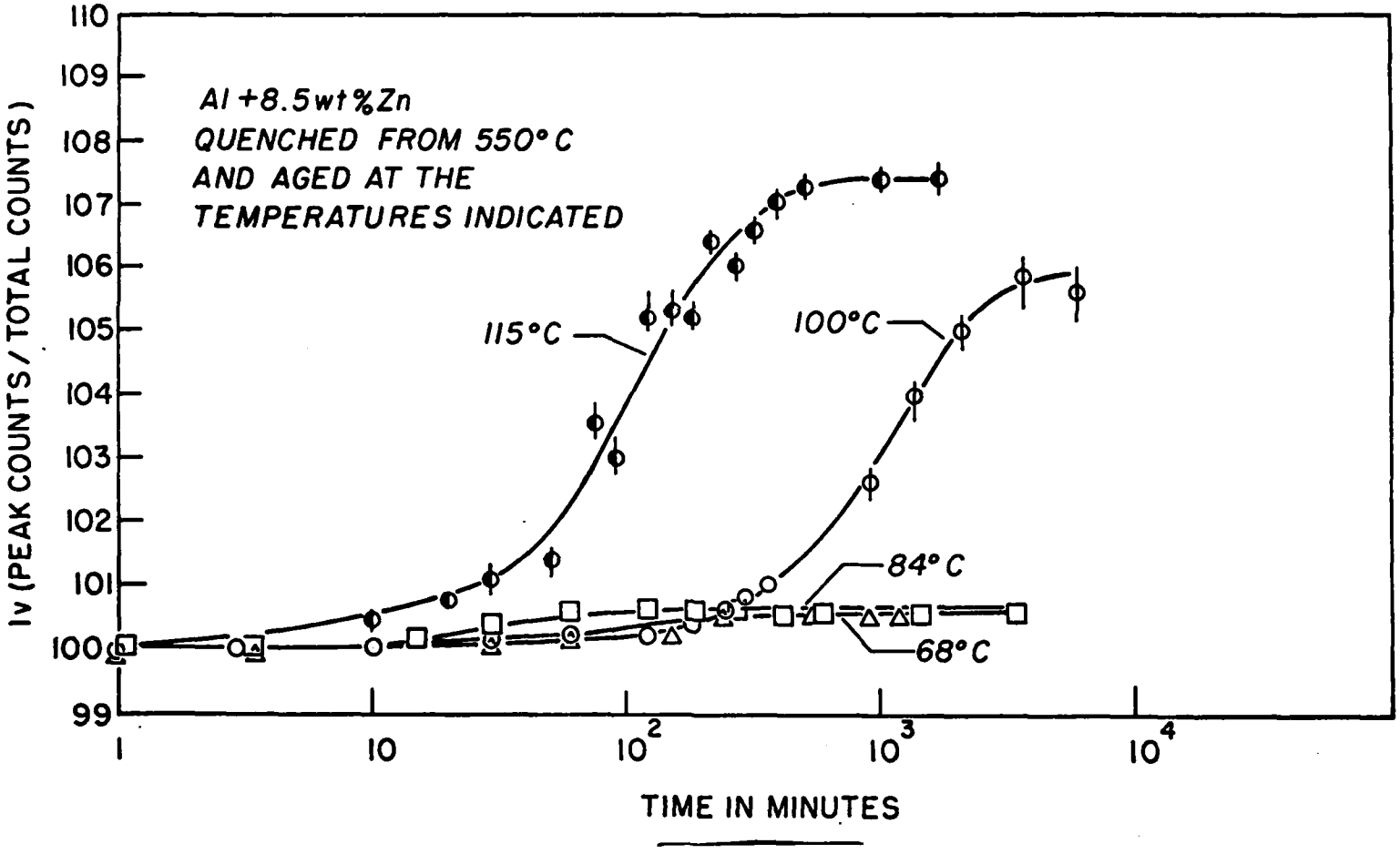
Al +8.5wt%Zn
QUENCHED FROM 550° C
AND AGED AT THE
TEMPERATURES INDICATED
115°C
100°C
84° C
68° C
Iv (PEAK COUNTS / TOTAL COUNTS)
110
109
108
107
106
105
104
103
102
101
100
99
1
10
10^2
10^3
10^4
TIME IN MINUTES

Figure 2 a

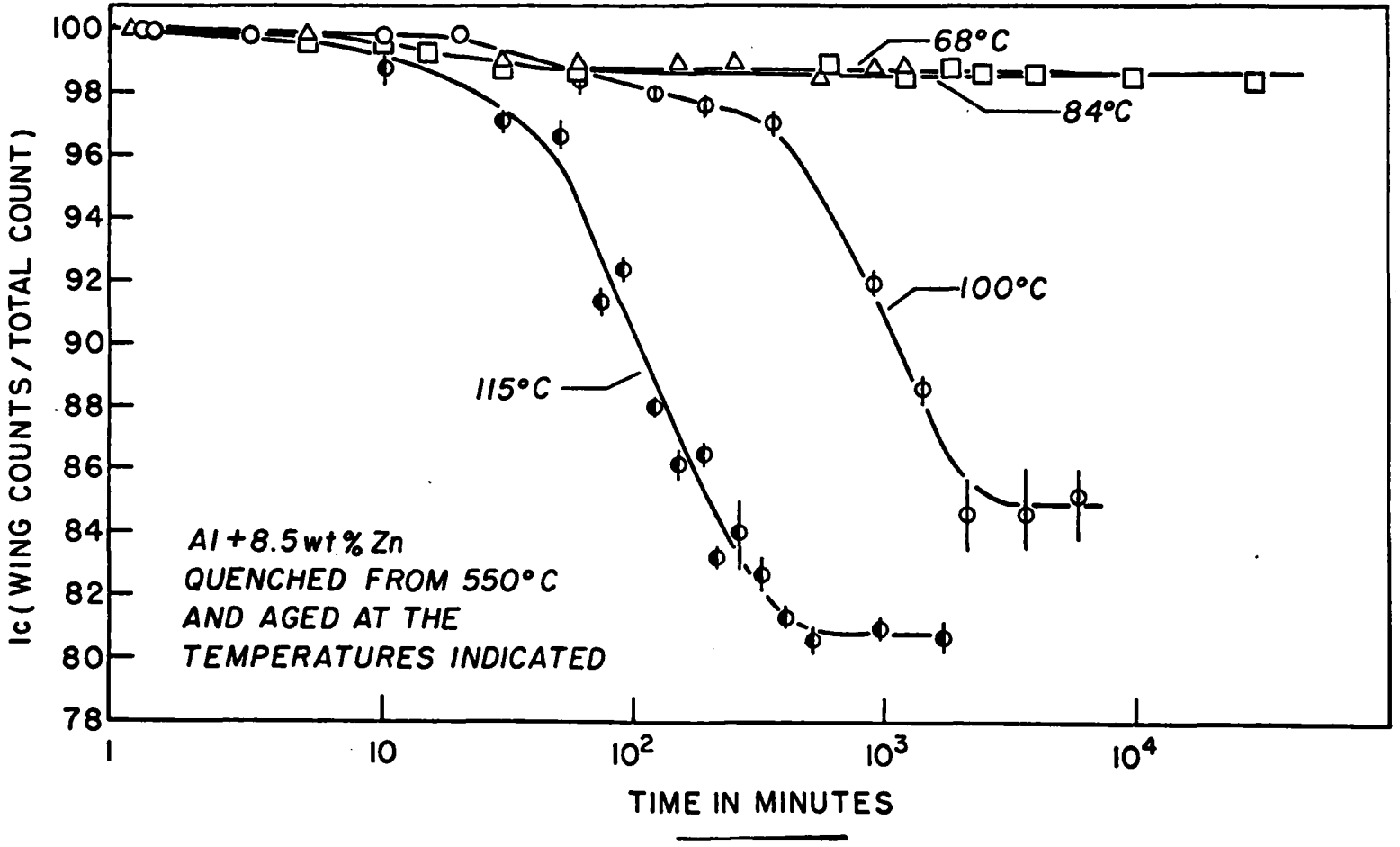
100
98
96
94
92
90
88
86
84
82
80
78
Ic( WING COUNTS / TOTAL COUNT )
68°C
84°C
100°C
115°C
Al + 8.5 wt % Zn
QUENCHED FROM 550° C
AND AGED AT THE
TEMPERATURES INDICATED
1
10
10²
10³
10⁴
TIME IN MINUTES

Figure 2 b

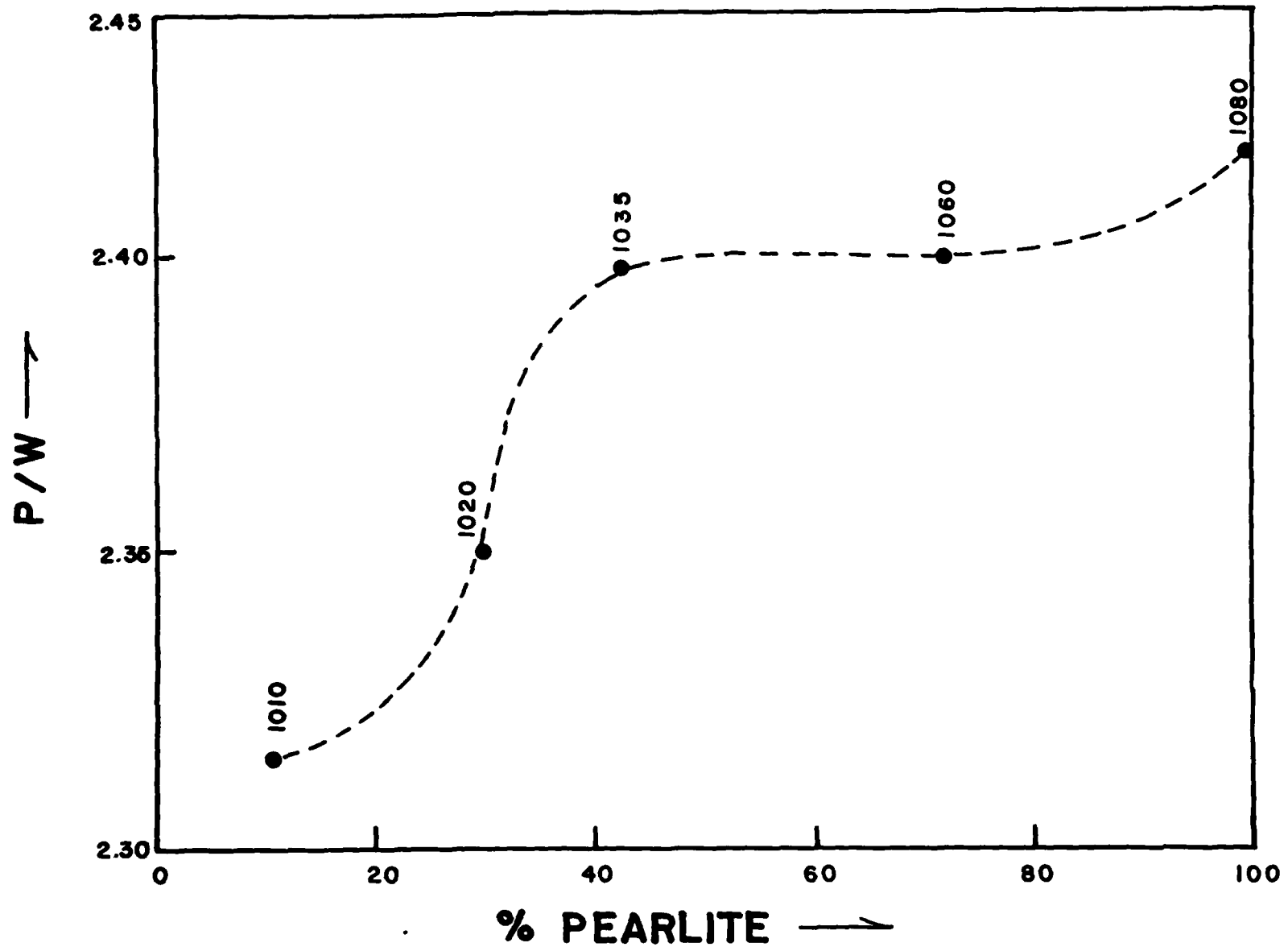
2.45
2.40
2.35
2.30
P/W
1010
1020
1035
1060
1080
0
20
40
60
80
100
% PEARLITE

Figure 3

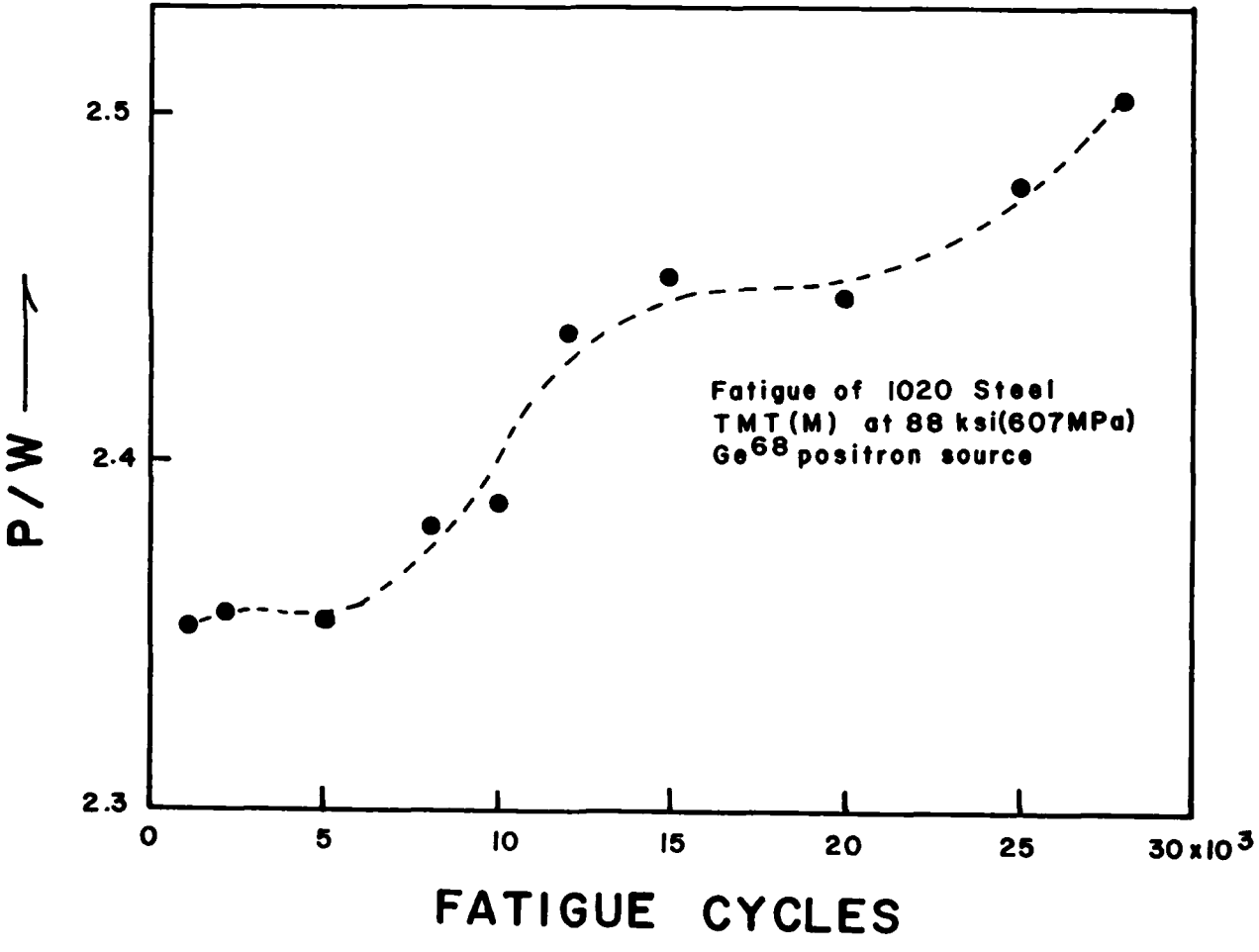
2.5
2.4
2.3
P/W
0
5
10
15
20
25
30x10³
FATIGUE CYCLES
Fatigue of 1020 Steel
TMT(M) at 88 ksi(607MPa)
Ge⁶⁸ positron source

Figure 4

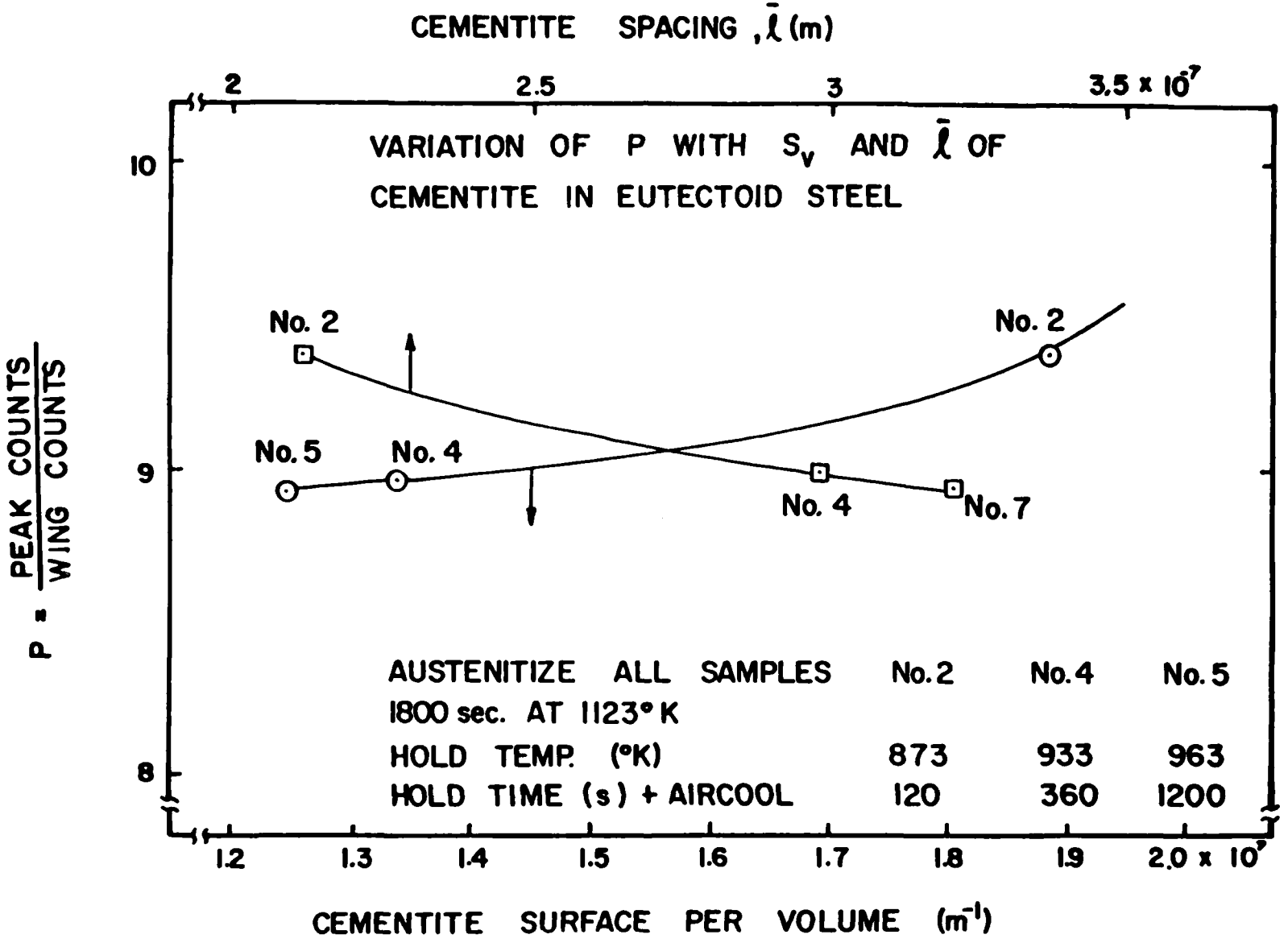
CEMENTITE SPACING , $\bar{\ell}$ (m)
2
2.5
3
3.5 x 10⁻⁷
VARIATION OF P WITH $S_v$ AND $\bar{\ell}$ OF
CEMENTITE IN EUTECTOID STEEL
No. 2
No. 2
No. 5
No. 4
No. 4
No. 7
10
9
8
P = PEAK COUNTS / WING COUNTS
AUSTENITIZE ALL SAMPLES
1800 sec. AT 1123° K
No. 2
No. 4
No. 5
HOLD TEMP. (°K)
873
933
963
HOLD TIME (s) + AIRCOOL
120
360
1200
1.2
1.3
1.4
1.5
1.6
1.7
1.8
1.9
2.0 x 10⁷
CEMENTITE SURFACE PER VOLUME (m⁻¹)

Figure 5

# The Trapping of Positrons by Dislocations Produced in Single Crystal Bending

M. L. JOHNSON, S. F. SATERLIE,
J. G. BYRNE

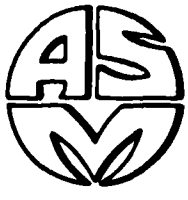


Reprinted from

METALLURGICAL TRANSACTIONS A
VOLUME 9A, NUMBER 6

Physical Metallurgy and Materials Science
JUNE 1978

# The Trapping of Positrons by Dislocations Produced in Single Crystal Bending

M. L. JOHNSON, S. F. SATERLIE, AND J. G. BYRNE

The deformation by bending of high purity copper and zinc single crystals was studied by detection and measurement of the Doppler-broadened gamma ray spectrum due to the annihilation of positrons in the crystals. The measurements were performed with a Ge(Li) spectrometer. The crystals were oriented and bent so as to introduce primarily edge dislocations into the material. The range of dislocation densities studied was from about $1.6 \times 10^9$ $m^{-2}$ to $1.3 \times 10^{12}$ $m^{-2}$.

Upon bending the copper crystals showed essentially a linear increase in shape factor (a parameter which describes the positron trapping) above a calculated dislocation density of $5 \times 10^{11}$ $m^{-2}$. The positron trapping rate per unit dislocation density was calculated from the experimental data and certain assumptions in the trapping model and found to be between $1.6 \times 10^{16}$ and $3.5 \times 10^{16}$ $s^{-1}$.

Annealing of the bent crystals is also discussed from the standpoint of the effect it has on the trapping of positrons. Polygonization produced an increase in shape factor which is attributed to trapping by low angle subgrain boundaries.

## 1. INTRODUCTION

POSITRONS can be utilized as sensitive probes of crystals. This is due to the fact that the positron causes negligible perturbation of the electronic structure in its passage through the crystal. Once a positron enters a solid it loses energy through electromagnetic interactions and quickly reaches the thermal energy of approximately kT which is 0.02 eV at room temperature. The positron is very susceptible to trapping at such a low kinetic energy. Every energy well it encounters which has a binding energy greater than kT is a possible trapping site.

Hodges[1] has calculated that a vacancy would represent a potential well of depth 10 eV on the average. A dislocation, however, theoretically represents a much smaller energy well. Edge dislocations have been theoretically modeled in aluminum as a two-dimensional square well by Martin and Paetsch.[2] Calculations of the depth of these square wells give estimates of the binding energy of edge dislocations ranging from 0.025 to 0.10 eV for narrow and wide edges respectively.

To date the experimental measurement of the trapping of positrons by dislocations has been done somewhat ambiguously. A great many measurements have been performed on crystals which had dislocations, vacancies, and precipitated impurities. Thus, it is not clear that the effect of pure edge dislocations on the trapping of positrons has been probed.

Copper single crystals have been placed in tension in the [100] direction and a calculated trapping rate by dislocations was determined by McKee, *et al.*[3] Unfortunately, their sample was annealed at 573 K to remove point defects. Such an anneal can precipitate impurities and vacancies at dislocations as well as cause thermally activated jog formation. All of these phenomenon can also trap positrons. It has been shown for copper single crystals by Siamoto, *et al*[4] that increased annealing temperature results in increased positron trapping.

Bending about a specific axis of a properly oriented single crystal produces primarily edge dislocations of one sign.[5] According to the theory[5] proposed and confirmed by many other workers,[6-9] the number of excess dislocations introduced by bending is proportional to the radius of curvature of the bend.

In this paper we will attempt to show the effect that the introduction of edge dislocations in copper and zinc single crystals has on the trapping of positrons.

## 2. EXPERIMENTAL TECHNIQUES

The gamma ray energy spectrum from the annihilation of positrons in a crystal is measured with a Ge(Li) spectrometer. The system utilized digital stabilization to help eliminate shifts in the gain and the zero level. The system was adjusted to have a gain of 50 eV per channel at a resolution of 1.24 keV full width half maximum (FWHM) at the total count rate used. The count rate maintained for each run was 14 kHz which, with accumulation times of 1000 s, yielded on the average about $2 \times 10^6$ counts in the experimental peaks. Total count rates were monitored using a linear ratemeter and deviations were held to ±2 pct. Complete details of the system are presented elsewhere.[10]

Changes in the spectrum of the annihilation photons are most evident in the peak and wing or tail regions of the spectrum.[11] A shape factor ($P/W$) was thus determined as the sum of the counts in the peak region divided by the total number of counts in the two wing or tail regions. It was these shape factors, determined for each run, that were compared to determine what changes the sample had undergone through bending. The exact locations used in the spectrum to delineate the peak and wings regions varied with different materials and will be specified for each material below.

M. L. JOHNSON is Staff Engineer, Browning Arms Co., Morgan, Utah 84050, S. F. SATERLIE is Staff Scientist, H. E. Cramer Co., Inc., Salt Lake City, Utah, 84108, and J. G. BYRNE is Professor of Materials Science and Engineering, University of Utah, Salt Lake City, Utah 84112.

Manuscript submitted June 30, 1977.


ISSN 0360-2133/78/0612-0841$00.75/0

Two positron sources were used in these experiments. One of the sources was $Ge^{68}$ which was diffused onto a $1 \times 10^{-3}$ m diam spot on a thin nickel foil.* About 86 pct of the positrons emitted by this source have a kinetic energy of 1.90 MeV. The second source used was $Na^{22}$ which had been sealed between two thin sheets of mylar. The positrons emitted by the $Na^{22}$ source have an energy of 0.55 MeV.

*Prepared by New England Nuclear, Boston, Massachusetts.

High purity single crystals of copper (99.999 pct) and zinc (99.999 pct) were oriented to specific crystallographic orientations using the Laue back reflection X-ray technique. After the crystals were oriented they were then carefully cut into the shape of parallelepipeds using an acid ($HNO_3$) saw and mill. Figure 1(*a*) shows a typical crystal before bending and Fig. 1(*b*) shows the orientation of the crystal in the four point bending device.

Each crystal was oriented and cut so that the preferred slip plane had a given angle, $\Phi$, with respect to the top surface of the beam and the preferred slip direction in the slip plane had essentially no component in the *x*-direction. If the crystal is now bent as shown in Fig. 1(*b*), nearly all of the deformation should lie in the preferred slip plane and utilize the preferred slip direction. According to the theory of Gilman,[12] the number of excess edge dislocations, *n*, introduced should then be given by

$$n = \frac{1}{R|\mathbf{b}|\cos\Phi} \qquad [1]$$

where *R* is the radius of curvature of the bend, $|\mathbf{b}|$ is the absolute value of the Burgers vector and $\Phi$ is the angle between the slip plane and the original *y*-axis of the crystal. Values of $|\mathbf{b}|$ and $\Phi$ for the zinc and copper crystals are given in Table I.

Ideally the preferred slip direction should have no component in the *x*-direction. This was not always attainable in actual practice. The largest departure from this was an *x*-component which was no more than four degrees out of the *y*-*z* plane. Cahn[5] found that small errors in orientation did not seem to interfere with the bending process.

Prior to bending, the crystals were polished and then etched. The crystals were then examined with an optical microscope and a scanning electron microscope to obtain a count of the dislocation etch pit concentration. The samples were then bent to various radii of curvature with several *P/W* measurements taken at each bending stage. The crystals were bent to about $3 \times 10^{-3}$ m which was the smallest radius of curvature attainable. Unfortunately, slight surface orientation changes precluded effective etching of the crystals after the last bend and no final count of the dislocation density was obtained. The crystals were, however, examined after the final bend and this confirmed that the slip was uniform and on the predicted slip plane. Comparisons of measured etch pit density in copper with theoretical values were done by Livingston[6] and found to be in agreement within about 30 pct. Others[7-9] have found the theoretical values of dislocation density to be within a factor of two of the measured values over a range of densities from $1 \times 10^{10}$ $m^{-2}$ to $1 \times 10^{11}$ $m^{-2}$ in other materials.

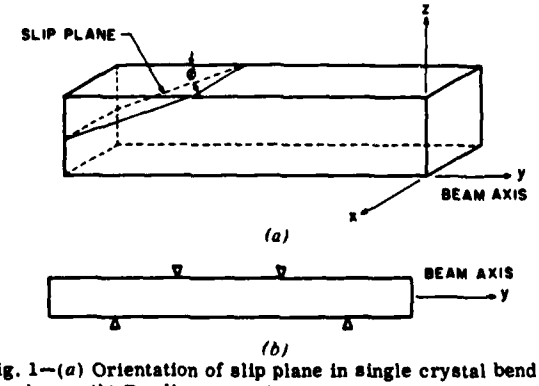


Fig. 1—(*a*) Orientation of slip plane in single crystal bend specimen. (*b*) Bending geometry.

Table I. Crystal Orientations Used and $|\vec{b}|$

| | Slip System Used | | $\Phi$ | Value of $|\vec{b}|$, m |
|---|---|---|---|---|
| Zinc | (0001) | $\langle\bar{2}110\rangle$ | 15 deg | $2.664 \times 10^{-10}$ |
| Copper | (111) | $\langle 110\rangle$ | 32 deg | $1.805 \times 10^{-10}$ |

## 3. EXPERIMENTAL RESULTS

### 3.1. Copper Single Crystal

The copper crystal was a parallelepiped with a width of $5 \times 10^{-3}$ m, a length of $3 \times 10^{-2}$ m, and a thickness of $1.5 \times 10^{-3}$ m. Measurements were taken of this crystal at a count rate of 14 kHz which gave a peak that contained about $2 \times 10^6$ counts for a 1000 s run. The source used for these runs was $Na^{22}$. The shape factor for these measurements was determined using the peak region of the spectrum (510 keV < E < 512 keV) and the two tail regions of the spectrum (506.8 keV < E < 509 keV and 513 keV < E < 515.2 keV).

The crystal was bent in stages until it had reached a radius of curvature of about $4 \times 10^{-3}$ m. This gave a dislocation density range of $4 \pm 2 \times 10^9$ $m^{-2}$ (found by etch pits) to $1.6^{+1.7}_{-0.5} \times 10^{12}$ $m^{-2}$ (calculated from Eq. [1]). The uncertainty in the higher dislocation density was obtained by using $2 \times 10^{-3}$ m as the uncertainty in the smallest radius of curvature. Three or four runs were taken of the sample at each radius of curvature. The source was repositioned slightly after each run to ensure that the average shape factor would be from slightly different parts of the crystal. In practice no inhomogeneities could be detected with different source positions giving nearly identical shape factors each time. The plot of the experimental shape factor (*P/W*) *vs* the dislocation density is presented in Fig. 2 for copper.

The copper crystal was annealed at high temperature to arrange the dislocations into polygon walls after the last stage of bending. This phenomenon has been studied in copper[13,14] and occurs at temperatures above 1173 K. The crystal was annealed at 1183 K in an argon atmosphere for various times ranging from 60 to $6.6 \times 10^3$ s. The crystal was always allowed to cool slowly to prevent the trapping of nonequilibrium numbers of vacancies although concurrent experiments with single crystal copper have shown that the trapping of positrons by these defects is not observa-

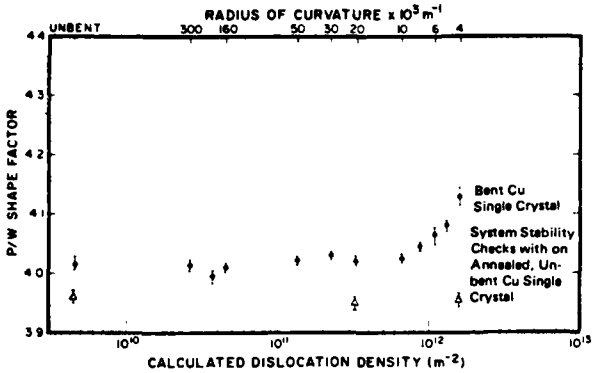


Fig. 2—The circular data points represent experimental Peak to Wings shape factor *vs* dislocation density calculated from the radius of curvature of the bent Cu single crystal. The triangular data points represent only system stability checks with an annealed, unbent Cu single crystal (these latter points, therefore, represent only the initial dislocation density of the crystal used in the stability checks).

ble at room temperature using either Doppler broadening or positron lifetime techniques.[15] The surface of the annealed crystal was also electropolished with a 60 pct $H_3PO_4$-40 pct $H_2O$ solution after each heating in order to eliminate any surface oxide formed during heating. The resulting *P/W* shape factors for each of the runs are shown in Fig. 3.

### 3.2. Zinc Single Crystal

The zinc crystal used was a parallelepiped of width $5 \times 10^{-3}$ m, length $2.5 \times 10^{-2}$ m, and a thickness of $1.5 \times 10^{-3}$ m. Measurements were taken as described for the copper, however, the $Ge^{68}$ source was used in these runs. The shape factor for these measurements was determined using the peak region of the spectrum (510.15 eV < E < 511.85 keV) and the two tail regions of the spectrum as (506.3 keV < E < 508.8 keV and 513.2 keV < E < 515.7 keV). The crystal was bent in stages until a radius of curvature of $3 \times 10^{-3}$ m was attained and the experimental shape factors are shown in Fig. 4.

The Zn crystal was annealed in argon gas for 2400 s at 653 K after bending in an attempt to polygonize it. It has been found earlier[5] that these conditions should be adequate to polygonize zinc. The shape factor after polygonization and electropolishing is also shown in Fig. 4. The range of dislocation density was from $1.6 \pm 2 \times 10^9$ m$^{-2}$ (from etch pits) to $1.3^{+3.0}_{-0.5} \times 10^{12}$ m$^{-2}$ (calculated from Eq. [1]). Again, the uncertainty at the higher dislocation density was obtained using $2 \times 10^{-3}$ m as the uncertainty in the smallest radius of curvature. The crystal was measured again after five days at room temperature and the shape factor for this measurement is included in the plot. An etch pit study of the zinc before and after the anneal revealed a uniform etch pit distribution before the anneal and a 70 pct polygonized structure after the anneal.

## 4. DISCUSSION AND CONCLUSIONS

Theoretical studies of the trapping of positrons by dislocations have always left some doubt about the effectiveness of the trapping. These current bending experiments on copper and zinc single crystals indicate that pure edge dislocations (the type primarily introduced in bending) can be detected above concentrations of about $5 \times 10^{11}$ m$^{-2}$. It is thought that screw dislocations are not effective traps for positrons.[11] Figure 5 is a plot of the *P/W* shape factor *vs* dislocation density above a dislocation density of $5 \times 10^{11}$ m$^{-2}$ obtained from the copper single crystal. A least squares fit of the data shows that to a correlation coefficient of 0.96 pct the curve fits the linear equation

$$y = 4.0 + 1.0 \times 10^{-13}\chi \qquad [2]$$

where $y$ is the shape factor and $\chi$ is the dislocation density in m$^{-2}$. This appears valid over the range of dislocation densities of $0.5 \times 10^{12}$ to $1.6 \times 10^{12}$ m$^{-2}$.

Using a method of analysis originated by McKee, *et al*,[3,16] the probability, $P_t$, that a positron will be trapped by a defect before annihilating can be shown to be directly related to changes in the shape factor, $S$, (synonomous with the *P/W* shape factor discussed in this paper) according to:

$$P_t = (S - S_f)/(S_t - S_f) \qquad [3]$$

where $S_f$ is the shape factor when none of the positrons are trapped (a fully annealed crystal), $S_t$ is the shape factor when 100 pct of the positrons are trapped (a highly deformed crystal), and $S$ is the shape factor at any defect concentration between 100 pct trapping and no trapping. The trapping probability can also be expressed as

$$P_t = \mu C/(\lambda_f + \mu C) \qquad [4]$$

where $\mu$ is the positron trapping rate per unit dislocation density (in units of s$^{-1}$), $C$ is the fractional concentration of dislocation cores, and $\lambda_f$ is the annihilation rate of untrapped positrons in the material. The concentration of dislocation cores, $C$, is obtained by dividing the number of dislocation lines emerging from each square meter of the crystal surface by the number of atoms on the surface in a square meter.

Eliminating $P_t$ from Eqs. [3] and [4] leaves the equation for the positron trapping rate as:

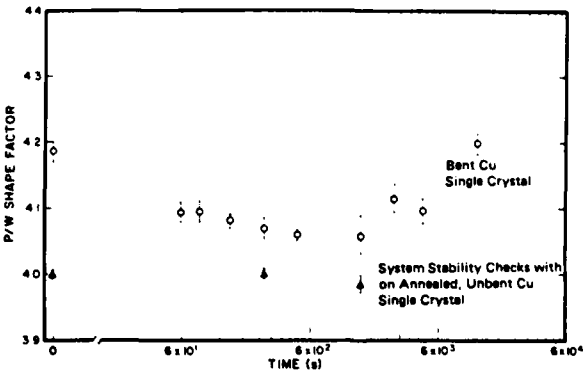


Fig. 3—The circular data points represent experimental Peak to Wings shape factor versus annealing time at 1183 K for Cu crystal after bending. The triangular points represent only system stability checks with an annealed, unbent Cu single crystal (these latter points, therefore, represent only the initial dislocation density of the crystal used in the stability checks).

$$\mu = \frac{\lambda_f}{C\{[(S_t - S_f)/(S - S_f)] - 1\}} \quad [5]$$

The average annihilation rate of untrapped positrons, $\lambda_f$, is $7.7 \times 10^9$ s$^{-1}$.[16] Copper has about $1.9 \times 10^{19}$ atoms per m$^2$ of surface. Once the shape factors at no trapping and complete trapping have been determined the positron trapping rate can be calculated.

McKee, *et al*[16] put copper single crystals into tension in the [100] direction and found a value of $\mu$ for dislocations assuming that all of the defects in the material were clean, straight dislocations. This assumption, however, is not completely clear especially after the 573 K anneal given the deformed material. Their calculated value of $\mu$ was found to be $2.9 \pm 1.0 \times 10^{15}$ s$^{-1}$.

Calculation of $\mu$ requires a knowledge of the saturation shape factor, $S_t$. In this bending experiment it did not appear that saturation was obtained. However, if it is assumed that all defects introduced by heavy rolling trap positrons in the same manner as dislocations, then a reasonable estimate of $S_t$ can be obtained. A shape factor of 4.60 was obtained from the Doppler measurements of a heavily rolled copper single crystal. This value will be used in the calculations as an estimate of the shape factor at 100 pct trapping. This corresponds to a dislocation density of about $6 \times 10^{12}$ m$^{-2}$ from Eq. [2]. This dislocation density would require bending the crystal to a radius of curvature of about $1 \times 10^{-3}$ m which was beyond our capability. The value of $S_f$ used was taken as the shape factor at zero bending. Using these in Eq. [5] gives the trapping rate per unit dislocation density from the bending data to be

$$\mu = 1.6 \pm 0.4 \times 10^{16} \text{ s}^{-1}.$$

McKee's group[16] claims a saturation value in positron lifetime measurements from their copper single crystal tension experiments which is about 50 pct of the value that is usually obtained in the rolling of copper. In terms of the shape factors for our experiment, this would give a saturation value, $S_t$, of about 4.3. This value used in Eq. [5] with the bending data from our experiment gives a positron trapping rate per unit dislocation density of

$$\mu = 3.5 \pm 0.1 \times 10^{16} \text{ s}^{-1}.$$

Thus, the value of $\mu$ is *not* a strong function of the value used for $S_t$. Both these calculated values of

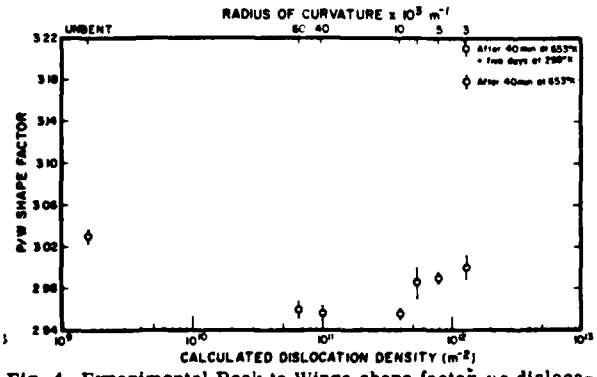


Fig. 4—Experimental Peak to Wings shape factor *vs* dislocation density calculated from radius for curvature of bend for zinc single crystal.

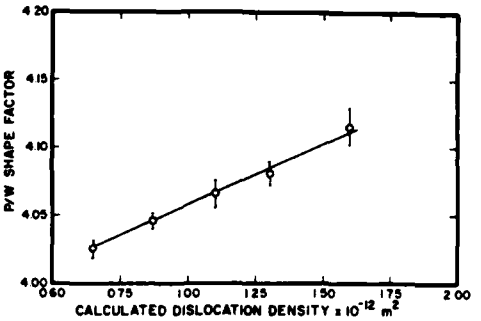


Fig. 5—Expanded plot of experimental Peak to Wings shape factor *vs* dislocation density calculated from the radius of curvature of bending for the Cu crystal.

the trapping rate for edge dislocations, however, are about ten times larger than McKee's estimate.

The current computed trapping rate of edge dislocations can be compared to that of vacancies using the data found by McGervey and Triftshauser.[17] They have experimentally determined the positron trapping rates for vacancies to be $1.37 \times 10^{14}$ s$^{-1}$. Because of the longer range distortion of the crystal lattice created by a dislocation they should be expected to trap positrons more efficiently than vacancies. This would be especially true if the positron is not as localized in the lattice as the earlier models of the positron indicated. The higher trapping rates by dislocations could also be due to the availability of more continuous bound states for positrons at a linear defect than at a point defect.[16]

The 1183 K annealing of the copper single crystal shown in Fig. 3 exhibits at $1.2 \times 10^4$ s a high trapping rate most likely caused by low angle grain boundaries. Cotterill, *et al*[18] point out that subgrain boundaries in Al are effective traps. Siamoto, *et al*[4] have shown evidence of this effect in single crystal copper tensile samples annealed at 773 K when compared to an anneal at 573 K. The last annealing stage ($1.2 \times 10^4$ s at 1173 K) in this experiment was also examined and it was found that numerous annealing twins were visible with the naked eye. Since the twin boundary area is very small compared to the area of polygon walls formed, it is very unlikely that the presence of twin boundaries would invalidate the explanation that the high shape factor observed for this last anneal is due to subgrain boundaries. Microscopic study of etch pits after the longest annealing time showed that polygon boundaries had formed over much of the bent crystal. The shape factor also showed an initial decrease which can be attributed to the annihilation of many dislocations of opposite sign. The final increase in shape factor occurs after polygon walls begin to form.

The shape factor *vs* radius of curvature for the Zn crystal is shown in Fig. 4. The initial decrease in shape factor probably comes from a slight decrease in the dislocation density of the initial high dislocation density clusters which were observed microscopically prior to bending. The initial bending strain may have been sufficient to break up the clusters, thus decreasing their effectiveness as traps. Above a theoretically calculated dislocation density of $5 \times 10^{11}$ m$^{-2}$, the shape factor begins to increase. Unfortunately, not enough data are available to do a detailed numerical analysis of the positron trapping in Zn.

The data point in Fig. 4 representing the 2400 s anneal of Zn at 653 K is very likely the result of enhanced positron trapping at subgrain boundaries after polygonization as was the case for the copper crystal. Because the melting point of zinc is 692.5 K, the 653 K anneal probably polygonized the zinc more completely than did the 1183 K anneal in copper whose melting point is 1356 K. The increased shape factor of the polygonized zinc after five more days at room temperature shows in Fig. 4 the possibility of continued dislocation climb. Climb in zinc at room temperature has been mentioned by various authors including Gilman[12] but has not been confirmed. Possibly positrons can be used to detect much smaller changes in dislocation arrangement than has been possible with other measurement techniques.

This paper has attempted to show the effect of trapping of positrons due to edge dislocations. Trapping rates per unit dislocation density were determined and found to be an order of magnitude higher than previously measured values. The trapping rate by dislocations also appears to be about a factor of one hundred larger than the trapping rate of vacancies. The trapping of positrons by low angle grain boundaries in copper single crystals and probably even dislocation climb in zinc at room temperature were observed. Thus, these experiments indicate that edge dislocations and groups of edge dislocations are effective traps for positrons and that this area merits further investigation.

## ACKNOWLEDGMENTS

The authors gratefully acknowledge the United States Air Force Office of Scientific Research for the support of this research. The authors also appreciate the valuable assistance of R. Waki in the development of the computer programs and for other experimental assistance.

## REFERENCES

1. C. H. Hodges: *Phys. Rev. Lett.*, 1970, vol. 25, p. 284.
2. J. W. Martin and R. Paetsch: *J. Met. Phys. F.*, 1972, vol. 2, p. 997
3. B. T. A. McKee, W. Triftshauser, and A. Stewart: *Phys. Rev. Lett.*, 1972, vol. 28, p. 358.
4. S. Siamoto, B. T. A. McKee, and A. T. Stewart: *Phys. Status Solidi*, 1974, vol. A21, p. 623.
5. R. W. Cahn: *J. Inst. Metals*, 1949, vol. 86, p. 121.
6. J. D. Livingston: *J. Appl. Phys.*, 1960, vol. 31, p. 1071.
7. P. Sinha: *J. Appl. Phys.*, 1961, vol. 32, p. 1222.
8. J. J. Gilman: *Acta Met.*, 1955, vol. 3, p. 277.
9. F. L. Vogel: *Trans. AIME*, 1956, vol. 206, p. 946.
10. M. L. Johnson: *M.S. Thesis*, University of Utah, 1977.
11. P. C. Lichtenburger: *Ph.D. Thesis*, 1972, University of Waterloo, Canada.
12. J. J. Gilman: *Micromechanics of Flow*, McGraw-Hill, 1969.
13. D. M. Shrader: *Phys. Rev.*, 1970, vol. A1, p. 1070.
14. A. G. Gould, R. N. West, and B. G. Hogg: *Can. J. Phys.*, 1972, vol. 50, p. 2294.
15. S. F. Saterlie, M. L. Johnson, P. Alexopoulos, and J. G. Byrne: unpublished research, University of Utah, 1977.
16. B. T. A. McKee, S. Siamoto, A. T. Stewart, and M. J. Stott: *Can. J. Phys.*, 1974, vol. 52, p. 759.
17. J. D. McGervey and W. Triftshauser: *Phys. Lett. A*, 1973, vol. 44, no. 1, p. 53.
18. R. M. J. Cotterill, K. Peterson, G. Trumpy, and J. Traff: *J. Phys. F.*, 1972, vol. 2, p. 459.

phys. stat. sol. (a) 48, 551 (1978)

Subject classification: 1.3 and 10.1; 21; 21.1

*Department of Materials Science and Engineering, University of Utah, Salt Lake City*

# The Removal of Defects from Solids as Observed with Positron Annihilation

By

M. L. JOHNSON, S. SATERLIE, D. BOICE, and J. G. BYRNE

The recovery, recrystallization and grain growth of cold rolled samples of Cu, α-brass, and Ni are followed with positron Doppler broadening and, in the case of Ni, positron lifetime measurements. The positron measurements show similar behavior during the annealing of cold worked metals as do hardness measurements, however, the positron measurements are quite sensitive to changes in the recovery region in which hardness is completely insensitive. Positron measurements are also much more sensitive than hardness measurements to detect the beginning of grain growth.

Die Erholung, die Rekristallisation und das Kornwachstum von kaltgerollten Proben von Kupfer, α-Messing und Nickel werden mit Positron-Doppler-Verbreitung und im Falle des Nickels auch mit Positronlebensdauermessungen verfolgt. Die Positronmessungen zeigen ähnliches Verhalten während der Wärmebehandlung des kaltgeformten Metalles wie die Härtemessungen, jedoch sind die Positronmesssungen verhältnismäßig empfindlich gegen Änderungen in der Erholungszone in welcher die Härte vollständig unempfindlich ist. Positronmessungen sind daher für die Bestimmung des Beginns des Kornwachstums sehr viel empfindlicher als Hartemessungen.

## 1. Introduction

One of the classic operations in solid state studies is that of annealing a cold worked material so as to cause in the material successive processes of recovery, recrystallization, and grain growth. Historically, it was customary to follow these three processes with observations of hardness, microstructure, and electrical resistivity. It is well known [1] that isochronal anneals at successively higher temperatures will not normally produce changes in the hardness or optical microstructure during the recovery range, although the electrical resistivity will decrease slightly during recovery. As the isochronal annealing temperatures increase, the recrystallization range is passed through and the hardness (as well as other macroscopic strength parameters) decreases drastically, and the optical microstructure reveals that new strain-free grains have nucleated and grown. Finally, at still higher temperatures the grain growth regime mostly produces progressively larger grain size in the optical microstructure.

It was the purpose of the current research to apply the measurement of a relatively new parameter, the Doppler energy broadening of the annihilation γ-ray energy, to the same classical processes. The annihilation γ-ray measured is that which accompanies the annihilation of a positron with some electron in the sample. The positron is injected via some convenient radioactive source such as $^{22}$Na or $^{68}$Ge placed close to the sample and on the opposite side of the sample from a Ge(Li) detector as described in detail elsewhere [2, 3].

Since it is established that defects in crystals do respond to positron measurements [4 to 7], the current work was intended to discover how similar or dissimilar to hardness measurements would be the response of positrons to the fairly complicated changes involved during annealing.

## 2. Experimental Procedure

The recovery, recrystallization, and grain growth of cold rolled polycrystalline samples of Cu, α-brass, and Ni were followed with positron Doppler broadening and, in the case of Ni, positron lifetime measurements. The Doppler broadening and positron lifetime experimental techniques have been described in detail elsewhere [2, 3]. All samples were polycrystalline and, in the case of Cu, two sets of samples were cold rolled to 10 and 50% thickness reductions, respectively. The α-brass samples were cold rolled to a 50% and the Ni samples to a 69% reduction in thickness. Separate samples for each reduction were annealed 1 h at each of a number of temperatures. Before and after annealing, positron and hardness measurements were made. The latter measurement is a more familiar way to follow recovery, recrystallization, and grain growth and was performed as a basis for comparison purposes.

## 3. Results and Discussion

The first information was taken on Cu rolled 10%. Fig. 1 shows the familiar hardness response to recovery, recrystallization, and grain growth stages and also the corresponding positron Doppler broadening response. One notices that the peak/wing (P/W) shape factor, which compares the central and wing areas of the Doppler peak [2], is not flat during recovery as is the hardness, but rather is quite sensitive to the recovery processes. In Fig. 1 one also sees that the start of the grain growth regime is clearly defined relative to the hardness, commencing at about 375 °C. Although the hardness continues to decrease during grain growth, this is not the case for the P/W parameter. If a higher degree of cold rolling (50%) is examined one finds in Fig. 2 that the start of recrystallization shifts as expected [1] to a lower temperature (250 °C).

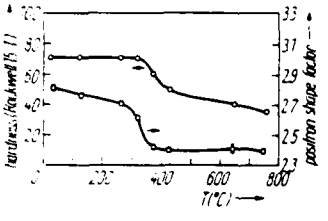


Fig. 1. Hardness and positron shape factor (peak wings — experimental) versus annealing temperature for copper cold rolled 10%

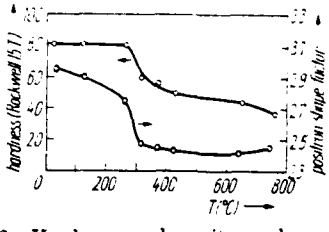


Fig. 2. Hardness and positron shape factor versus annealing temperature for copper cold rolled 50%

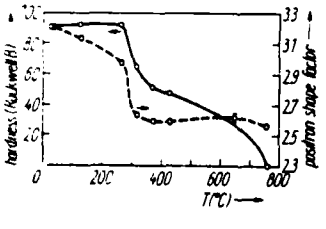


Fig. 3. Hardness and positron shape factor versus annealing temperature for α-brass cold rolled 50%

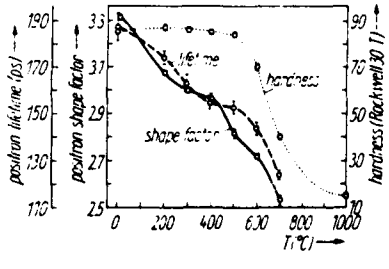


Fig. 4. Hardness, positron shape factor, and positron lifetime versus annealing temperature for nickel cold rolled 69%

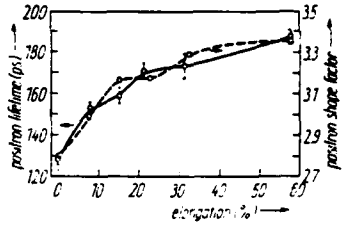


Fig. 5. Positron lifetime and positron shape factor versus percent tensile elongation for nickel

In Fig. 2, one sees that the P/W ratio has a larger change in the recovery region than for the 10% deformed samples described in Fig. 1. Also, as in Fig. 1, one can see in Fig. 2 that the start of grain growth is much more clearly indicated by the Doppler data curve than by the hardness curve. As before, the hardness continues to drop during grain growth whereas the P/W ratio remains fairly constant.

Fig. 3 shows the hardness behavior of α-brass rolled 50%. If the initial hardness of the 50% rolled Cu shown in Fig. 2 is converted to the hardness scale used in Fig. 3 one gets a value of 59 Rockwell B, indicating the Cu is considerably softer for the same amount of cold rolling than is the α-brass. This higher hardness is due to the lower stacking fault energy of the α-brass relative to the Cu, which leads to a higher work hardening rate. The comparisons of hardness and positron behavior for the α-brass are very similar to those already made for the Cu. The major difference is that the P/W data for the recovery region for the α-brass seen in Fig. 3 show even a larger change than for the 50% cold worked Cu seen in Fig. 2.

Ni cold rolled 69% is described in Fig. 4, which contains curves for hardness, P/W ratio, and positron lifetime. The positron measurements were not performed on specimens annealed above 700 °C, and hence they do not include the grain growth regime. The main difference of the Ni behavior from that of the Cu and α-brass behavior is that the transition from recovery into recrystallization is not as distinguishable in the nickel samples. Further, the curvatures are more complicated in the P/W and positron lifetime curves for Ni than they were for either Cu or α-brass.

Finally, if the positron lifetime and shape factor data on the tensile deformation of Ni in Fig. 5 are examined it can be seen that both positron measurements show similar behavior as would measurements of the flow stress [8] (i.e. a general increase with increasing elongation or increasing damage in the material).

## 4. Conclusions

The measurements of positron Doppler broadening and positron lifetime show similar unique differences from hardness measurements during the annealing of cold worked metals. Both positron measurements are quite sensitive to changes in the recovery region in which hardness is completely *insensitive* and both positron measurements are much more sensitive than hardness measurements to the beginning of the grain growth region.

***Acknowledgements***

The positron Doppler broadening work was supported by the U.S. Air Force Office of Scientific Research. The positron lifetime measurements were supported by the U.S. Energy Research and Development Administration.

## References

[1] J. G. BYRNE, Recovery, Recrystallization, and Grain Growth, Macmillan, New York 1965 (p. 34).
[2] S. SATERLIE, M. L. JOHNSON, P. ALEXOPOULOS, F. SEPPI, R. URE, and J. G. BYRNE, phys. stat. sol. (a) 41, K75 (1977).
[3] K. G. LYNN, C. M. WAN, R. W. URE, and J. G. BYRNE, phys. stat. sol. (a) 22, 731 (1974).
[4] M. L. JOHNSON, S. SATERLIE, and J. G. BYRNE, Metallurg. Trans. 9A, 841 (1978).
[5] J. H. KUSMISS, A. N. GOLAND, and C. L. SNEAD, JR., phys. stat. sol. (b) 50, 33 (1972).
[6] R. M. J. COTTERILL, K. PETERSON, G. TRUMPY, and J. TRAFF, J. Phys. F 2, 459 (1972).
[7] A. A. ADMENKO, Y. YA. DEKHTYAR, and V. S. MIKHALENKO, Soviet Phys. – Doklady 13, 702 (1969).
[8] P. B. HIRSCH and T. E. MITCHELL, Work Hardening, Gordon & Breach, New York 1968 (p. 65).

*(Received March 16, 1978)*

**short note**

reprinted from

**physica**
**status**
**solidi (a)**

phys. stat. sol. (a) 42, K175 (1977)

Subject classification: 10.1; 21

Department of Materials Science and Engineering, University of Utah

# Positron Measurements of Aging in Complex Aluminum Alloys

By

M.L. JOHNSON, S. PANCHANADEESWARAN, S. SATERLIE, and J.G. BYRNE

This communication is the first report of the application of the technique of positron annihilation to precipitation hardening in complex commercially important aluminum alloys. The particular positron measurement used was that of the Doppler energy broadening /1/ of the gamma photons which accompany the annihilation of positrons with electrons. This Doppler effect is reflective of the energy of the electron involved in the annihilation and is being used to an increasing extent /2/ to characterize damage in solids. In order to describe changes in the Doppler broadening, the parameter we report is a shape factor which characterizes the distribution curve of the energy values about the value of 511 keV, the energy of the annihilation photon from an event involving an electron at rest. The shape factor is a ratio of the area under a central region of the peak to the area under the wing portion of the peak. A material with a higher defect density is associated with a higher peak/wing shape factor, (P/W), because a positron trapped at a vacancy or dislocation, for example, has a higher probability of eventually annihilating with a conduction electron than with a core electron. This would result in a small Doppler shift from 511 keV because the conduction electron has a lower momentum than a core electron. Both positive and negative shifts from 511 keV occur since the center of mass of the annihilation pair may be moving in any direction at the time annihilation occurs.

The first material studied was 2024 alloy, of nominal composition 4.4% Cu, 1.5% Mg, 0.6% Mn, and balance Al (all in wt%). Specimens were solution treated at 493 $^{o}$C, water quenched and aged at 190 $^{o}$C for times up to 10 h. The samples were kept in liquid nitrogen except when being measured. In Fig. 1 one sees that the Doppler (P/W) ratio increases during aging and levels off in much the same way as does the yield strength. Increasing hardness or yield strength in a material indicates increasing damage or defect density which increases the P/W shape factor.

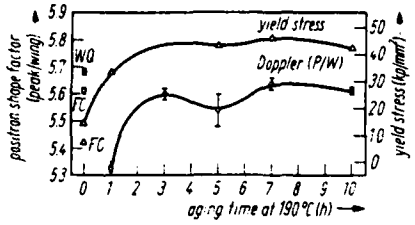


Fig. 1

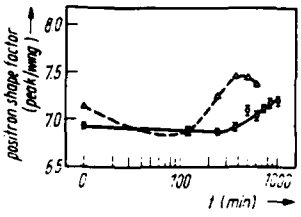


Fig. 2

Fig. 1. 0.2% offset yield stress and positron Doppler experimental peak/wing shape factor versus aging time at 190 °C for 2024 aluminum alloy after solution treatment at 493 °C, WQ: water quenched; FC : furnace cooled

Fig. 2. Positron Doppler experimental peak/wing shape factor versus aging time at 130 °C for 7075 aluminum alloy after solution treatment at 480 °C; ——aging after 5% cold rolling, – – – aging directly after water quenching

The as-quenched (WQ) P/W value in Fig. 1, however, is noteworthy since it is much higher than the P/W value for 1 h of aging. We know it is not the result of surface damage from the quench because electropolishing preceded the P/W measurement. It may, however, be similar to earlier measured effects /3/ in which 2024 alloy in a shot peened condition was quenched from 500 °C and showed a 6.97% increase in P/W shape factor. It is perhaps fortuitous that, from Fig. 1, the ratio of P/W factors between the WQ and 1 h aged conditions is 6.67%, however, the likelyhood exists that a solute-vacancy trapping mechanism is operative on quenching this material. When the 190 °C aging begins this situation would rapidly be modified as precipitation commences. The high P/W value after furnace cooling is at about the same level as is the P/W aging curve at 8 h. This is reasonable since slow furnace cooling typically produces an overaged condition.

Fig. 2 shows the behavior of another important age hardening alloy, 7075, which consists of 5.6% Zn, 2.5% Mg, 1.6% Cu, 0.3% Cr, and balance Al. The dashedcurve shows an aging maximum at 500 min for aging at 130 °C after quenching. As for 2024, we see a higher P/W value for the quenched condition than for the first aged condition and again we can eliminate surface damage as the cause of

this since the samples were etched with a NaOH solution and cleaned with an $HNO_3$ solution after quenching and prior to measuring the P/W ratio. The main point of Fig. 2, however, is that the quenched solid solution, rolled 5% prior to aging, shows a retardation of aging kinetics. This was described by Conserva et al. /4/ as due to the nucleation of coarser precipitates on the dislocations created by the rolling. In addition to being coarse, the precipitates are said /4/ to exhibit preferential growth directions, to take advantage of the dislocation arrangement. This situation, at least in 7075, is not favorable to general hardening. Thus the precipitates enhance positron trapping, but it is not clear whether this trapping is a consequence of the coherency strains which exist around the precipitates or is associated with the precipitate matrix interface. The latter interface, as it becomes less coherent upon overaging, is frequently described in terms of interface dislocations. Thus it is most likely that the trapping occurs either at the interface, when dislocations or pseudo-dislocations are involved, or close to the interface when coherence produces a highly strained region without dislocations. Another factor involved in the trapping of positrons at precipitate particles is that most of the atoms in the precipitate region contribute fewer conduction electrons ($Cu^{1+}$, $Mg^{2+}$, $Mn^{2+}$) than do atoms of the Al rich matrix. The precipitate thus appears less positive to a positron than does the matrix, hence attracts and traps the positron.

In conclusion, positron measurements can faithfully represent changes in the aged state of commercially important precipitation hardening alloys.

Acknowledgement

The authors appreciate the support of the Air Force Office of Scientific Research during this research.

References

/1/ R.N. WEST, Positron Studies of Condensed Matter, Taylor and Francis Ltd., London 1974.

/2/ J.G. BYRNE, AFML-TR-75-212, 695 (1975).

/3/ M.L. JOHNSON, P. ALEXOPOULOS, S. SATERLIE, and J.G. BYRNE, unpublished data, 1977.

/4/ M. CONSERVA, M. BURATTI, E. DIRUSSO, and F. GATTO, Mater. Sci. Engng. 11, 103 (1973).

(Received June 20, 1977)

# short note

reprinted from

physica
status
solidi (a)

phys. stat. sol. (a) 48, K83 (1978)

Subject classification: 1.3 and 10.1; 21

Department of Materials Science and Engineering,
University of Utah, Salt Lake City

# Positron Trapping at Precipitates in Aluminum-4 wt% Copper Single Crystals

By

S. PANCHANADEESWARAN, R.W. URE, Jr., and J.G. BYRNE

The course of age hardening in aluminum base alloys has frequently been studied by utilizing the classical aluminum base copper system /1/. During early aging in this system, planar Guinier-Preston zones (called GPI and GPII) /2/ are produced. These GP zones have high coherency strains and dislocations must cut through them rigidly in order to pass on /3/. Subsequent aging results in softening generally associated with the development of a transition precipitate $\Theta'$ and finally an equilibrium precipitate $\Theta$. Both $\Theta'$ and $\Theta$, which may be by-passed rather than cut by dislocations /3, 4/, exhibit decreasing lattice coherency strains, produce a lower yield stress, and greatly raise the rate of work hardening during plastic deformation /3/.

Positron annihilation /5/ has recently been applied to many materials studies, such as fatigue /6, 7/, phase transformations /8/, cold-work /9 to 11/, radiation damage /12, 13/, hydrogen embrittlement /14/, etc. In this paper, we describe results of positron annihilation observations on aluminum-copper alloys during various stages of solid state precipitation hardening.

Single crystals of Al-4wt% Cu were grown by the strain anneal technique /3/ and heat treated as described in Table 1.

Table 1

Thermal treatments and resultant precipitates or pre-precipitates.
Solution treatment of 1 h at 550 °C and a water quench preceeded all treatments

| aging treatment | result |
|---|---|
| 1. none, as water quenched | supersaturated solid solution |
| 2. 130 °C for 48 h | GPI zones, pre-precipitate |
| 3. 190 °C for 5 h | GPII zones, pre-precipitate |
| 4. 240 °C for 24 h | $\Theta'$, transition precipitate |
| 5. 400 °C for 24 h pus 205 °C for 48 h | $\Theta$, equilibrium precipitate |

The positron experiments consisted of measuring the Doppler broadening of the energy of the annihilation photon which accompanies the electron-positron annihilation event /8, 11/. If the electron which combines with the positron to annihilate it were "at rest", the gamma particles emitted would have an energy of 511 keV. However, the electrons are not at rest and consequently the gamma particle which is emitted may have energy larger or smaller than 511 keV due to the Doppler shift. This energy difference is, on average, larger in an annealed or more defect-free material than in a cold worked or otherwise damaged material. The reason for this behavior is that a positron trapped at a defect sees fewer high energy core electrons since ions are missing in such regions. The annihilations then occur more often with lower momentum electrons causing smaller Doppler energy shifts from the central 511 keV value. The exact converse is true for materials containing few defects.

Pre-precipitate particles such as GPI and GPII zones have coherent long range strain fields around them. Transition precipitates ($\Theta'$) and equilibrium precipitate particles ($\Theta$) have progressively smaller long range strain fields and more of a high angle grain boundary type interface between themselves and the matrix. All of the above entities have a chemical difference with the matrix. The quenched condition is known to possess a combination of line and point defects as well as copper atoms in solid solution. The positron annihilation experiments reported here were aimed at trying to determine how much positron interactions with the line and point defects occur.

The annihilation photon energies were measured with a lithium drifted germanium detector. The circuit and technique have been described in detail elsewhere /15/. The parameter which is used to describe changes in a material is the peak/wings shape factor (P/W). A sharpening of the Doppler curve (increase in P/W ratio) indicates some form of internal damage or strain in the sample and conversely. Two positron sources were utilized, $^{22}$Na and $^{68}$Ge. $^{22}$Na produces positrons with a maximum energy of 0.546 MeV and $^{68}$Ge produces positrons with a maximum energy of 1.9 MeV. Thus the germanium data are acquired over a greater penetration depth than are the sodium data. Using the density of Al and the above mentioned values of $E_{max}$ for the two sources, the theory of Brandt/16/ gives positron penetration depths of $9.04 \times 10^{-5}$ m for $^{22}$Na and $5.46 \times 10^{-4}$ m for $^{68}$Ge.

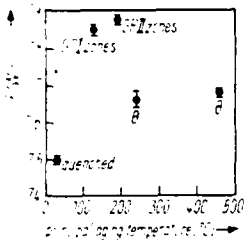


Fig. 1

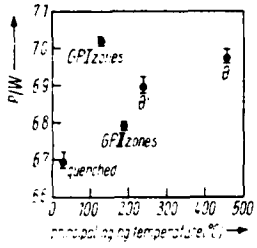


Fig. 2

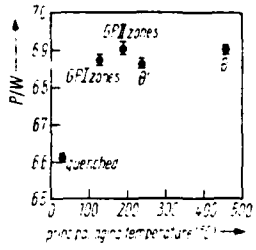


Fig. 3

Fig. 1. Doppler peak to wings (P/W) shape factor versus aging temperature for an Al + 4 wt% Cu single crystal. Data taken using a $^{22}$Na positron source

Fig. 2. Doppler peak to wings (P/W) shape factor versus aging temperature for an Al + 4 wt% Cu single crystal. Data taken using a $^{68}$Ge positron source

Fig. 3. Doppler peak to wings (P/W) shape factor versus aging temperature for polycrystalline Al-4 wt% Cu material. Data taken using a $^{68}$Ge positron source

Fig. 1 shows how the P/W ratio values for a single crystal region close to the exterior surface vary with progressive age hardening. The values rise from the quenched value and pass through a maximum. The data of Fig. 2 obtained with the $^{68}$Ge positron source are similar (except for the GPII data point) and lie in a generally lower magnitude range. When the experiment was repeated with polycrystalline alloy material, the data of Fig. 3 were obtained. These data are similar to those of Fig. 2 but are generally slightly lower point for point (again with the exception of GPII).

A number of important conclusions may be drawn from comparing the three figures. First of all for the "bulk" data obtained with $^{68}$Ge, the polycrystalline P/W values are usually lower for each condition than the corresponding P/W values for the single crystal experiments. This would indicate that in the quenched condition fewer point defects are present in the polycrystal because of leakage to grain boundary sinks. In subsequent aging, this defect density difference would lead to a lower density of precipitate nucleation sites in the polycrystal /17/. This would account for the lower P/W ratios in a GP zone condition because the coherency strain or hardness of the region measured would be lower. Again the GPII single crystal $^{68}$Ge

data point violates this scheme. This same data point will later be seen to be at variance with a $\Theta'$ discussion and so should reasonably be regarded as a bad data point although the reason is presently not known. When one considers the $\Theta'$ and $\Theta$ conditions the lower nucleation frequency again can be used to explain the lower P/W values for the polycrystalline samples. However, the basis for the values themselves is no longer coherency strains but reflects positron trapping at the matrix particle interface.

A second conclusion is that the P/W values obtained nearer the external surface (by using $^{22}$Na) are in every case larger than those averaged over a greater depth ($^{68}$Ge data). This results from the higher quenching rate which occurs closer to the surface. For this reason the regions closer to the surface should exhibit higher defect concentrations after quenching and higher rates of precipitate nucleation during aging. This accounts for the greater P/W ratios for quenched, GP zone and overaged conditions.

In all regions (surface or deeper) the quenched P/W values are much smaller than either the GP zone or overaged conditions. This implies that the strain effect of GP zones is much more interactive with positrons than is the discrete point defect distribution created by quenching. The $\Theta'$ and $\Theta$ particle distributions are also more interactive with positrons than is the quenched state, but to a lesser degree than for the zone conditions. The reasons are different, i.e. incoherent particle-matrix interface reasons rather than strain field trapping of positrons.

It is usually true (again the suspect GPII $^{68}$Ge data point is the only exception) that the "defect" trapping of positrons is greater for GPII zones than for GPI zones. This would be in accord with the maximum hardness associated with the GPII condition chosen /1, 3/.

As one passes from a peak hardness (GPII) condition to $\Theta'$, the P/W ratio generally decreases (same exception as noted above). This indicates that positrons are less effectively trapped by the partially coherent interface of the $\Theta'$ particles than by the large strain fields of the coherent GPII particles.

Finally, it is always observed that when the system passes from partially coherent to completely incoherent particles the P/W ratio increases. Evidently, the completely incoherent $\Theta$ particle-matrix interface is a more effective positron trap than the

partially coherent $\theta'$ particle-matrix interface.

Acknowledgement

This research was sponsored by the Air Force Office of Scientific Research.

References

/1/ A. KELLY and R.B. NICHOLSON, Progr. in Mater. Sci. 10, No. 3 (1963).

/2/ A. GUINIER, Ann. Phys. (France) 12, 161 (1939).

/3/ J.G. BYRNE, M.E. FINE, and A. KELLY, Phil. Mag. 6, 1119 (1961).

/4/ J.C. FISHER, E.W. HART, and R.H. PRY, Acta metall. 1, 336 (1953).

/5/ R.N. WEST, Positron Studies of Condensed Matter, Monographs on Physics, Vol. 8, Taylor and Francis Ltd., London 1974.

/6/ K.G. LYNN, C.M. WAN, R.W. URE, and J.G. BYRNE, phys. stat. sol. (a) 22, 731 (1974).

/7/ K.G. LYNN and J.G. BYRNE, Metallurg. Trans. 7A, 604 (1976).

/8/ M.L. JOHNSON, S. PANCHANADEESWARAN, S. SATERLIE, and J.G. BYRNE, phys. stat. sol. (a) 42, K175 (1977).

/9/ K.G. LYNN, R. URE, and J.G. BYRNE, Acta metall. 22, 1075 (1974).

/10/ B. NIELSEN and K. PETERSEN, Fourth Internat. Conf. Positron Annihilation, Helsingør (Denmark) 1976 (p. 128).

/11/ P.C. LICHTENBERGER, C.W. SCHULTE, and I.K. MACKENZIE, ibid. (p. 133).

/12/ J.H. EVANS, O. MOGENSEN, M. ELDRUP, and B.N. SINGH, ibid (p. 71).

/13/ N. THRANE, K. PETERSEN, and J.H. EVANS, ibid. (p. 94).

/14/ F. ALEX, T.D. HADNAGY, K.G. LYNN, and J.G. BYRNE, Effect of Hydrogen on Behavior of Materials, Met. Soc. AIME 1975 (p. 642).

/15/ M.L. JOHNSON, S. SATERLIE, and J.G. BYRNE, Metallurg. Trans., in the press (1977).

/16/ W. BRANDT, Appl. Phys. 5, 1 (1974).

/17/ J.G. BYRNE, Scripta metall. 2, 477 (1968).

(Received April 7, 1978)

**short note**

reprinted from

**physica**
**status**
**solidi (a)**

phys. stat. sol. (a) 41, K75 (1977)

Subject classification: 12.1; 21

Department of Materials Science and Engineering, University of Utah, Salt Lake City

# Positron Annihilation Observations of Shot Peened Aluminum Alloys

By

S. SATERLIE, M.L. JOHNSON, P. ALEXOPOULOS, F. SEPPI, R. URE, and J.G. BYRNE

Positron annihilation techniques are being used to an increasing extent to study various types of damage in crystalline materials. A growing body of data exists for damage caused by irradiation with neutrons and electrons, fatigue, quenching, and plastic deformation. The present note describes positron effects noted for the important metal surface treatment called shot peening. The results and their interpretation are limited, since only particular samples were available. However, it is hoped that reporting the effects will encourage further studies in this vein because firstly, both shot penning and positron annihilation are uniquely concerned with surfaces rather than with interior regions, and secondly because positron annihilation offers a non-destructive monitoring possibility for the important surface peening treatment. The depth of the plastic deformation from peening is typically 0.4 mm /1/ whereas the depth of penetration of positrons in Al is typically less than 0.05 mm /2/ thus all of the positrons were annihilating well within the region of damage from the peening.

Samples of two aluminum alloys, 7075 and 2024, whose nominal compositions in weight percent are respectively: 1.6 Cu, 2.5 Mg, 0.3 Cr, 5.6 Zn and 4.4 Cu, 0.6 Mn, 1.5 Mg, were used to examine the damage done by surface shot peening. The main experimental techniques used to survey the damage were the measurements of the mean positron lifetime /3/ and the measurement of the Doppler broadening /4/ of the $\gamma$-ray photons which accompany the annihilation. In some instances the compressive residual stress /5/ in the surfaces of the peened specimens was measured by X-ray diffraction.

The 7075 alloy was in the T6 condition which signifies solution heat treatment and artificial aging to maximum hardness. The 2024 alloy was in the T3 condition, which signifies solution heat treatment followed by cold work. Before describing the re-

sults obtained it might be helpful to call the readers attention to the fact that an upper limit of detectability or saturation range exists for following the increase in defect density with positron annihilation measurements /6 to 9/. This limit exists because after a certain population of line and point defects have been put into a solid, all the positrons put into the sample are trapped and annihilated at defects, thus any subsequent increase in the defect population remains undetected for a given strength of positron source and detection system.

The positron source for the studies of the Doppler broadened positron annihilation spectrum was $Ge^{68}$ and counts were accumulated for 1000 s at a total count rate of $(20.0 \pm 0.1)\times10^3$ counts/s.

The positron annihilation peaks obtained in each run contained on the average about $3.0\times10^6$ counts. The experimental spectra were deconvoluted using a resolution spectrum determined from $Sr^{85}$ $\gamma$-rays. The Ge: Li spectrometer system used for the measurements had a resolution of 1.37 keV FWHM at the total count rate used. The gain of the system was 0.050 keV per channel. A shape factor was determined by summing the total number of counts in the central part of the spectrum (510 keV< < energy (E) < 512 keV) and dividing this by the total number of counts in two tail regions of the spectrum (507.5 keV < E < 508.9 keV and 513.1 keV < E < 514.5 keV). The positron source for the positron lifetime measurements was $Na^{22}$ and the lifetime circuitry was described elsewhere /10/. Both alloys were shot peened to an Almen intensity /11/ of 12.

The 2024-T3 alloy showed a large change in Doppler shape factor between that for the un-peened state ($7.38 \pm 0.07$) and that for the peened state ($7.65 \pm 0.02$). When a peened region was measured one year after peening the shape parameter was $7.56 \pm 0.06$ . In terms of positron lifetime: the values were 201 ps before peening, 223 ps after peening and 209 ps after one year of relaxation.

For the 7075-T6 alloy the Doppler shape factor of the unpeened material was $7.71 \pm 0.04$. When observed one year after peening no appreciable change had occurred ($7.72 \pm 0.06$). A once peened region was re-peened and re-measured the same day and a very slight increase in the Doppler shape factor to $7.81 \pm 0.06$ was observed. After peening positron lifetime measurements showed no appreciable increase above the unpeened value of $(218 \pm 2)$ ps. The X-ray measured compressive

residual stress after peening was 343 MN $m^{-2}$. This value relaxed to 314 MN $m^{-2}$ over a three month period and no further relaxation of residual stress occurred within a fifteen month period after peening.

In summary, 2024-T3 is quite sensitive to positron measurements of damage caused by shot peening when compared with 7075-T6 alloy. Aside from the compositional differences between the two alloys, the main reason for the insensitivity of the 7075-T6 to positron measurements is very likely the presence of a fully developed state of precipitation hardening as denoted by the T6 coding. This condition could easily have placed the 7075-T6 alloy into the saturation range /6 to 9/ for positron measurements before the shot peening was done. In this range the fraction of incoming positrons trapped at defects is so large, that a subsequent increase in defect density (as for example by shot peening) can affect that fraction only very slightly. In the case of the 2024-T3 the state of precipitation hardening (solution heat-treated and cold worked) is much less developed since only natural aging at ambient temperatures is involved. Clearly the cold work used in the T3 condition did not bring the 2024-T3 alloy above the upper limit of detectability for positron trapping prior to peening. Further support for this interpretation is the fact that some residual stress relaxation was detected by X-ray line shift measurements in the 7075-T6 alloy. Such stress relaxation is only effected by a recovery process. Thus some recovery indeed did occur but was not detectable in this case by positron measurements. This type of insensitivity to positrons has been seen often in similar situations /6 to 9/ where a cold worked state is far into the saturation range for positron trapping at defects.

## Acknowledgements

The authors greatfully acknowledge the Air Force Office of Scientific Research for support of the Doppler broadening measurements and the Energy Resources Development Administration for support of the positron lifetime measurements. The assistance of R. Waki was greatly appreciated.

## References

/1/ B.D. BOGGS and J.G. BYRNE, Metallurg.Trans. 4, 2153 (1973).

/2/ W. BRANDT, Proc. 3rd Internat. Conf. Positron Annihilation, Springer-Verlag, Berlin 1973 (p. 1).

/3/ R.N. WEST, Positron Studies of Condensed Matter, Monographs on Physics, Taylor and Francis Ltd., London/Barnes/Noble (N.Y.) 1974 (p. 8).

/4/ R.N. WEST, ibid. (p. 12).

/5/ A.L. CHRISTENSON and E.S. ROLAND, ASM Trans. 45, 638 (1953).

/6/ B.T.A. MC KEE, A.G.D. JOST, and I.K. MAC KENZIE, Canad. J. Phys. 50, 415 (1972).

/7/ J. BARAM and M. ROSEN, phys. stat. sol. (a) 16, 263 (1973).

/8/ G. DLUBEK. O. BRÜMMER, and E. HENSEL, phys. stat. sol. (a) 34, 737 (1976

/9/ T.D. HADNAGY, Ph. D. Thesis, University of Utah, 1976.

/10/ K.G. LYNN, C.M. WAN, R.W. URE, and J.G. BYRNE, phys. stat. sol. (a) 22. 731 (1974).

/11/ J.O. ALMEN, Metal Prog. 43, 209 and 270 (1943).

(Received March 17, 1977)

ARPA/AF Review of progress in quantitative NDE 1979

# A REVIEW OF RECENT POSITRON ANNIHILATION NDE APPLICATIONS

S. Panchanadeeswaran, Po-We Kao, R. W. Ure, Jr., and J. G. Byrne
Department of Materials Science and Engineering
University of Utah
Salt Lake City, Utah 84112

## ABSTRACT

This review will treat two recent applications of positron annihilation to metallurgical studies and will involve the measurement of the Doppler effect associated with the gamma rays emitted during positron annihilation. The applications will be: studies of the interactions of dislocations with pre-precipitates in aged Al-4 weight percent Cu single crystals and studies of the effect of hydrogen charging into polycrystalline nickel.

## Introduction

Earlier[1] it was reported that a commercial aluminum base age hardening alloy, 7075, responded to Doppler broadening measurements by exhibiting higher values of the peak to wings shape parameter for harder conditions. Thus, the Doppler shape factor was behaving in much the same way in which it would respond to plastic deformation in a pure metal; that is, in a pure metal subjected to damage the Doppler peak shape becomes sharper because dislocations and vacancies provide locations for positron trapping which are lacking in ion cores. Hence, positrons attracted to and trapped in such regions will tend more to annihilate with lower energy conduction electrons. Such annihilations cause a smaller Doppler shift from the central energy value of 511 keV than would be caused were the positron to annihilate with a more energetic core electron. Thus, the curve representing the number of annihilations versus plus and minus deviations in annihilation gamma ray energy about a central value of 511 keV (the value if the electron-positron center of mass were stationary) sharpens with rising defect concentration and, conversely, the shape broadens with the annealing out of damage. The gamma rays emitted on annihilation enter a Ge(Li) spectrometer capable of measuring their energy.

## Results

To have a better chance of understanding the response of positrons to changes during age hardening[2], we set out to produce well documented aged states in a known alloy; that is, to look at G. P. zones, transition precipitates (θ'), and the equilibrium precipitate (θ) in both single and polycrystalline Al + 4 weight percent Cu alloy. The heat treatments used were: solution treated (S.T.) at 550°C for 1 hour + water quench (Q) for the supersaturated solid solution; S.T. + Q + 130°C for 48 hours for G.P. I zones; S.T. + Q + 190°C for 5 hours for G.P. II zones; S.T. + Q + 240°C for 24 hours for θ'; and S.T. + Q + 400°C for 24 hours + 315°C for 48 hours for θ (the equilibrium precipitate).

When peak to wing (P/W) Doppler comparisons were made, both $Na^{22}$ and $Ge^{68}$ were used as positron sources. The $Na^{22}$ produces positrons with a maximum energy of 0.546 MeV and the $Ge^{68}$ produces positrons with a maximum energy of 1.9 MeV; thus, the former positrons will sample events closer to the specimen surface than the latter positrons.

P/W data for an aged single crystal utilizing a $Na^{22}$ positron source are shown in Fig. 1, plotted against the principal aging temperature. One sees a rise in P/W ratio from the solid solution level to the G.P. zone conditions and a later decline as θ' and θ are formed.

Figure 2 exhibits P/W data taken on the same samples, but with $Ge^{68}$ as the positron source. One sees a similar trend (except for the G. P. II point) in the data, all of which lie in a lower magnitude range. When these experiments were repeated with polycrystalline samples and the $Ge^{68}$ positron source, similar data trends to those of Fig. 2 resulted (with the exception of G. P. II).

A number of conclusions emerge at this point. For the "bulk" data obtained with $Ge^{68}$, the P/W values for the polycrystals were usually lower point for point than the corresponding values for the single crystal experiments. This would suggest that in the quenched condition fewer point defects are present in the polycrystal because of leakage to grain boundary sinks. In subsequent aging this would lead to a lower density of pre-precipitate nucleation sites in the polycrystal. This would account for the lower P/W ratios in a G. P. zone condition because the coherency strain or hardness of the region measured would be lower.

Again, the case of the G. P. II zone containing single crystal $Ge^{68}$ data violates this scheme. The same data point will later be seen to be at variance with the interpretation given to the θ' condition; that is, it can reasonably be regarded as a bad data point, but for reasons as yet unclear.

For θ' and θ data, the lower nucleation frequency again seems to explain the lower values of P/W ratio for the polycrystalline samples. However, the basis for the values themselves no longer can be ascribed to coherency strains, but rather may be reflective of positron trapping at the θ' and θ matrix-particle interface.

In every case, P/W values measured closer to the surface ($Na^{22}$) exceeded those measured at greater depths ($Ge^{68}$). This may be related to the higher quenching rates and point defect concentrations of the surface region which in turn would on aging produce a higher nucleation rate

of precipitate.

Independent of depth, the quenched solid solution was always lower in P/W ratio than either the G. P. zone or overaged conditions. This implies that the stain effect of G. P. zones is much more interactive with positrons than is the discreet point defect distribution created by quenching. The θ' and θ conditions are also more interactive with positrons than is the quenched state--again probably due to interfacial rather than strain field trapping reasons.

In comparing G. P. I and G. P. II zones, it seems (with the one exception previously noted) that the trapping of positrons is greater for the more highly stained G. P. II condition. As one then passes to the partially coherent (less strain) θ' situation, the positrons are less effectively trapped than by the coherent G. P. II particles. Finally, in comparing θ' and θ, it seems that the completely incoherent θ particles have a more effective positron trapping interface than do the θ' particles.

We now proceed to more recent single crystal experiments[3] in which the interaction of various of the above aged states in single crystals respond to tensile deformation. It is known that for G. P. zone states dislocations must rigidly cut through the zones[4], giving the crystal a high yield strength, but a modest rate of work hardening. For the θ' and θ situations, on the other hand, the dislocations bow out between the particles, wrap around, and pass on as in the Fisher-Hart-Pry[5] or Orowan[6] descriptions. The latter produces low initial strength, but a high rate of work hardening as multiple dislocation loops about the particles produce stress fields which resist the approach of new dislocations.

Figure 3 shows plots of Iv (the ratio of peak counts to total counts) and Ic (the ratio of wing counts to total counts) versus tensile strain for a G. P. I zone containing single crystals. The most important feature is that Iv does not change with tensile strain; that is, the cutting of G. P. I zones does not show up in Doppler broadening as would ordinary tensile strain. Ic changes appreciably only in the first 5 percent tensile strain. For G. P. II zone containing single crystals, Iv in Fig. 4 shows little but scatter once the initial 5 percent strain is completed.

For crystals containing the transition precipitate θ' and the equilibrium precipitate θ, the Doppler behavior is dramatically different from that for G. P. zones as might be expected from the very different deformation mechanisms involved. For example, for θ' containing crystals, both Iv and Ic respond quite rapidly to tensile strain as shown in Fig. 5. Again, for crystals containing the equilibrium precipitate θ, Fig. 6 shows a lesser magnitude, but an equally rapid response than for θ'.

The main distinguishing feature we seem to be seeing is that the cutting of G. P. zones does not appreciably change the positron response, but the operation of Fisher-Hart-Pry[5] or Orowan[6] work hardening mechanisms definitely does cause a positron response. The reason suggested is that positrons trap at the dislocations which wrap around the θ' and θ particles, but do not respond moving dislocations.

The second subject to be discussed is the hydrogen charging of metals[7]. Earlier work[8] in this laboratory showed a hydrogen-positron relationship in steel which was appropriate for the non-destructive detection of hydrogen embrittlement. In the subsequent work[8], nickel (after various amounts of cold work) was cathodically charged with hydrogen. The sharpness of the Doppler peak increased at first and to a greater extent the greater the amount of initial deformation. Following the initial sharpening, a broadening occurred. A mechanism which could explain this is one in which protons migrate to dislocations introduced by cold work and subsequently form gaseous hydrogen molecules which produce enough pressure to generate new dislocations at these locations. The broadening of the Doppler peak, following the initial narrowing, is attributed to protons reducing the attractive potential between positrons and dislocations. Figure 7 shows the undulating character of the positron-proton-dislocation relationship for two current densities for samples deformed 10.7 percent in tension.

A 70 percent cold rolled sample was cathodically charged for three hours and then measured as a function of time at 300°K. Figure 8 shows how P/W increased during this period. This is attributed in part to the diffusion of protons out of the sample. This would unscreen some dislocations and thus raise P/W. Another cause may be that protons detrapped from dislocations or delivered by dislocation short-cut diffusion to inclusions or grain boundary locations may combine to form $H_2$ and generate new dislocations by exerting pressure.

Figure 9 shows a schematic diagram of microhardness measurement directions on special samples. The central impression was made with a 1 kg load and the two orthogonal directions enabled 25 gram microhardness measurements to be made as a function of distance from the large impression with and without hydrogen charging. Figure 10 shows on the upper curve ($H_1$) how the microhardness varies with distance from a high dislocation density after charging and after a one hour anneal at 365°K (curve $H_2$); that is, with no charging.

Cathodic charging produced no change in the P/W shape factor of annealed Ni; yet, the microhardness of annealed Ni increased with charging as is seen by the right end of curve $H_1$ (higher than right end of curve $H_2$). This suggests that the P/W ratio was seeing an exact balancing between defect generation and defect screening by protons during charging. Yet, the existence of the defects could be seen via microhardness.

## Acknowledgements

The authors wish to acknowledge the financial support of the Air Force Office of Scientific Research which made this work reported in this review possible.

1. M. L. Johnson, S. Panchanadeeswaran, S. Saterlie, and J. G. Byrne, Phys. Stat. Sol. (a) 42, 175 (1977).

2. S. Panchanadeeswaran, R. W. Ure, Jr., and J. G. Byrne, Phys. Stat. Sol. (a) 48, 83 (1978).

3. S. Panchanadeeswaran, unpublished results (1979).

4. J. G. Byrne, M. E. Fine, and A. Kelly, Phil. Mag. 6, 1119 (1961).

5. J. C. Fisher, E. W. Hart, and R. H. Pry, Acta. Met., 1, 336 (1953).

6. E. Orowan, A Symposium on Internal Stresses (London: Inst. of Metals), 451 (1948).

7. *Po-We Kao, R. W. Ure, Jr., and J. G. Byrne,* Phil. Mag. (a) 39, 517 (1979).

8. F. Alex, Ph.D. thesis, University of Utah (1976).

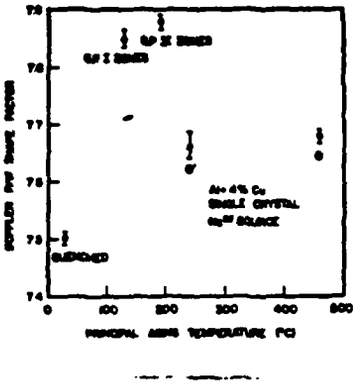

Fig. 1. Doppler P/W shape factors for an Al + 4 percent Cu single crystal in various aged states. $Na^{22}$ positron source.

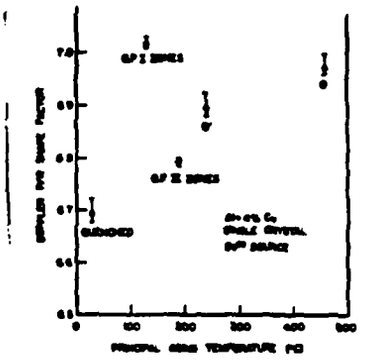

Fig. 2. Doppler P/W shape factors for an Al + 4 percent Cu single crystal in various aged states. $Ge^{68}$ positron source.

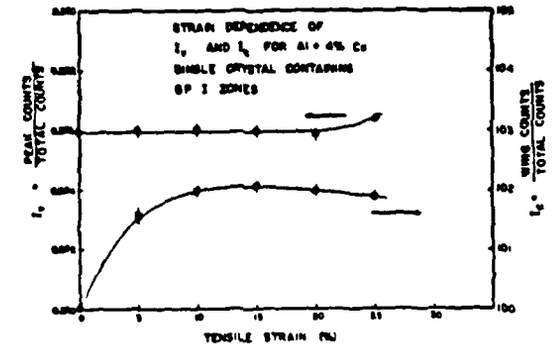


Fig. 3. Doppler peak to total (Iv) and wings to total (Ic) shape factors versus tensile strain for an Al + 4 percent Cu single crystal containing G. P. I zones.

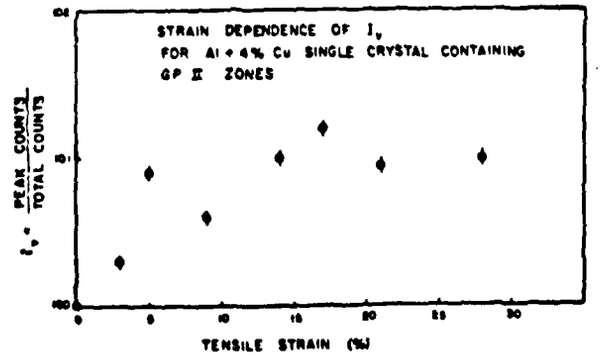


Fig. 4. Doppler peak to total (Iv) shape factor versus tensile strain for an Al + 4 percent Cu single crystal containing G. P. II zones.

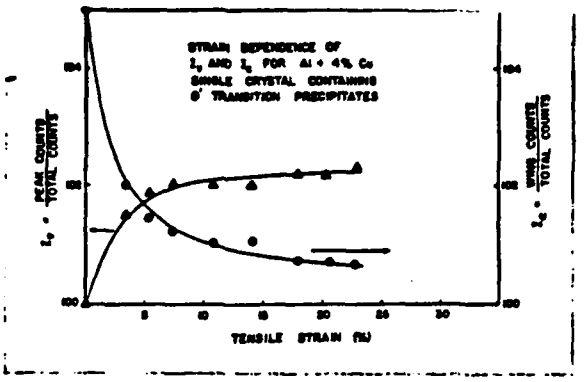


Fig. 5. Doppler peak to total (Iv) and wings to total (Ic) shape factors versus tensile strain for an Al + 4 percent Cu single crystal containing θ' transition precipitates.

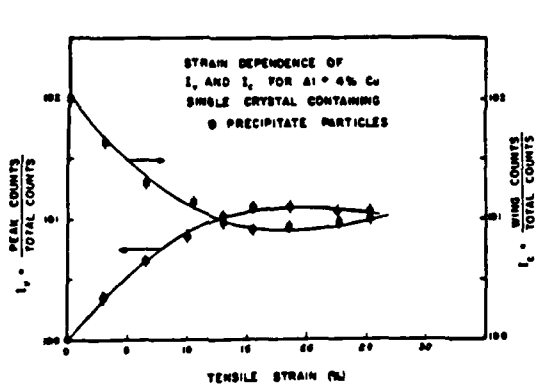


Fig. 6. Doppler peak to total (Iv) and wings to total (Ic) shape factors versus tensile strain for an Al + 4 percent Cu single crystal containing θ equilibrium precipitate particles.

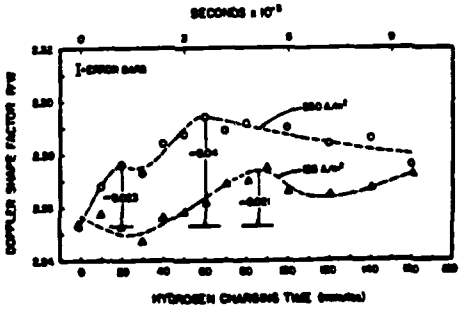


Fig. 7. Doppler peak to wings shape factor versus hydrogen charging time in polycrystalline nickel.

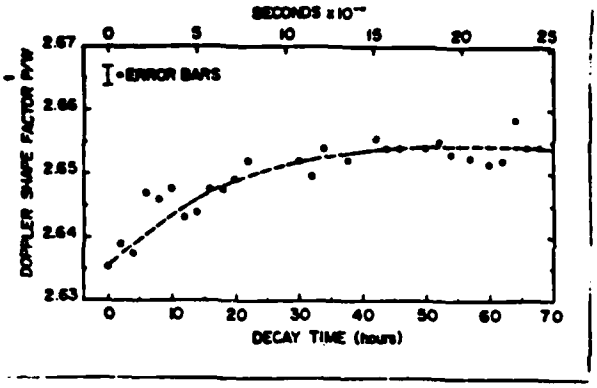


Fig. 8. Doppler peak to wings (P/W) shape factor versus decay time at ambient following cathodic charging of hydrogen into nickel.

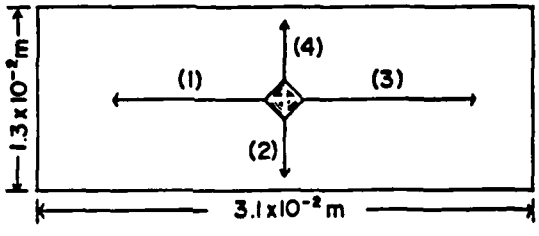


Fig. 9. Microhardness measurement directions and sample size for results shown in Fig. 10. Paths 1 and 2 could be used before and paths 3 and 4 after cathodic charging.

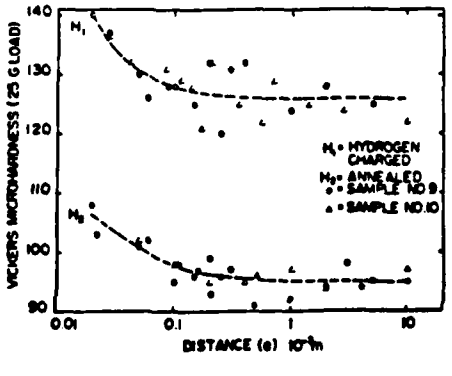


Fig. 10. Microhardness versus distance from a 1,000 gm impression before (curve $H_2$) and after (curve $H_1$) cathodic charging of hydrogen into nickel.

PHILOSOPHICAL MAGAZINE A, 1979, VOL. 39, NO. 4, 517–527

# A study of hydrogen charging of nickel by positron Doppler broadening

By PO-WE KAO, R. W. URE, JR., and J. G. BYRNE
Department of Materials Science and Engineering, University of Utah, Salt Lake City, Utah 84112, U.S.A.

[Received 19 July 1978 and accepted 16 November 1978]

ABSTRACT

The cathodic charging of hydrogen into polycrystalline nickel has been studied by measurements of the Doppler energy shifts of gamma-rays emitted during positron annihilation in the samples. In general, the annihilation photopeak initially narrows with hydrogen charging, indicating an increase in defect density. The extent of this photopeak narrowing increases with the amount of cold work prior to hydrogen charging. A mechanism is proposed in which dissolved hydrogen (protons) migrate to dislocations introduced by cold work and subsequently form gaseous hydrogen molecules and/or nickel hydride particles which have enough pressure and/or lattice misfit, respectively, to produce structural damage in the form of new dislocations at those locations. The broadening of the Doppler peak following the initial narrowing is attributed to protons reducing the attractive potential between positrons and dislocations. The results show that positrons can be an effective tool with which to study hydrogen in solids.

## § 1. INTRODUCTION

Hydrogen is absorbed by most metals either during fabrication or service and often causes component failure after prolonged periods at stresses within normal load-bearing capabilities. The importance of this problem of hydrogen embrittlement is increasing in energy-related technology. The current paper focuses on some fundamental questions related to this problem by studying proton interactions with defects by positron annihilation. For example, what are the proton trapping sites? In the absence of externally applied load, what is the role of dislocations in hydrogen embrittlement?

An earlier study showed that the positron-lifetime technique can be used to study hydrogen embrittlement of 4340 steel (Alex, Hadnagy, Lynn and Byrne 1975). Hydrogen charging produced positron trapping and annihilation at defects. However, in specimens initially in a highly cold-worked state, hydrogen charging caused a decrease in the degree of positron trapping and annihilation at defects. It was suggested by Alex *et al.* (1975) that this measured decrease in positron lifetime was a result of protons trapped at these defects thereby reducing the attractive potential between the defects and positrons, i.e. a proton screening effect of the defects since protons as well as positrons are attracted to and trapped by defects with negative effective charge. The initial increase of positron lifetime during hydrogen charging was taken to imply that plastic deformation can be generated by the hydrogen. Indeed, it has been clearly shown (Wampler, Schober and Lengeler 1976) that

copper in which hydrogen bubbles were formed had dense tangles of dislocations around the bubbles as well as arrays of prismatic dislocation loops ejected from the bubbles. The current work utilized nickel rather than steel in order to test the earlier mentioned positron-related ideas in a material that is structurally less complex than steel.

When an energetic positron from a suitable radioactive decay enters condensed matter, it rapidly loses almost all of its kinetic energy (thermalizes) and eventually annihilates with an electron producing two gamma-rays in the dominant decay mode. The thermalized positron is assumed to be at rest when annihilation occurs. Hence, the momentum of the electron–positron centre of mass and the resultant gamma-ray energy depend mainly on the momentum of the electron with which the positron annihilates. From these gamma photons one can obtain information on the electron density and momentum. Three measurements have been developed to analyse these annihilation photons: positron lifetime, the angular distribution (correlation) of the gamma-rays, and the Doppler broadening of the annihilation gamma energies. A thorough review of all three techniques has been written by West (1973).

In the investigation of defects in metals by means of positron annihilation, the positive charge of the positron interacts with the potential near a defect in a crystal. This leads to a reduced probability of the positron staying near defects with an effective positive charge and an increased localization of the positron at defects with an effective negative charge. The latter type of defect constitutes a potential well for the trapping of the positron which is very susceptible to such trapping. The theoretical foundation of the trapping model was reviewed by Seeger (1974). Once a positron is trapped at such a defect the probability is high that it will annihilate with a lower-energy conduction electron, since ion cores with their higher-energy electrons are lacking in the defect region.

## § 2. Experimental

The positron source used was $^{68}$Ge electroplated onto one side of a nickel foil. The nickel foil was $10^{-4}$ m thick and the entire source was enclosed in polyethylene sheet about $5 \times 10^{-5}$ m thick to prevent contamination. A complete description of the Doppler broadening system as well as the source-sample configuration was presented earlier (Johnson 1977, Johnson, Saterlie and Byrne 1978). There are several ways to analyse the electron momentum profiles obtained from positron annihilation. In lineshape techniques (Lichtenberger 1974) one examines the number of counts within certain regions of the momentum spectrum. A number of ways are available to define the lineshape. For example, with reference to fig. 1, one may compare areas within various energy (channel number) ranges such as central region to total, wing regions to total or central to wing regions. The first indicates the fraction of conduction- (and low momentum core-) electron annihilations, the second the fraction of high momentum core-electron annihilations and the last the ratio of conduction- and low momentum core- to high momentum core-electron annihilations. In the present work the latter was used, i.e. the Peak/Wings (P/W) lineshape factor.

Fig. 1

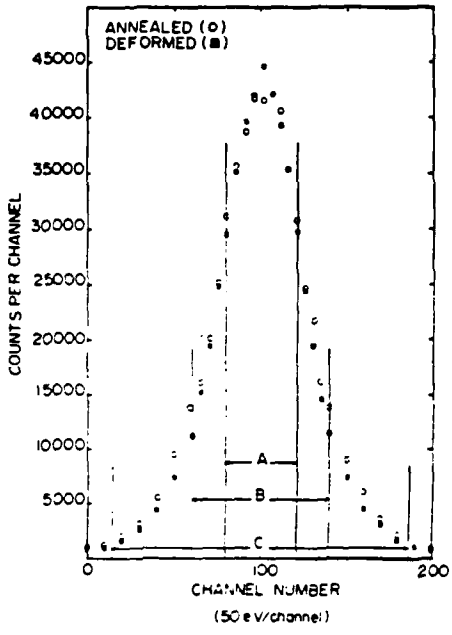


Typical Doppler-broadened annihilation spectrum of nickel.

The specimens are made from nickel which contained major impurities of 0·93 wt.% Fe, 0·028 wt.% Cu and 0·017 wt.% Co. Specimens were studied representing the 70% cold-rolled condition and various tensile strains applied at a strain rate of $3 \times 10^{-4}$ s$^{-1}$. All of these deformations were preceded by a 1 hour anneal at 973 K in an argon atmosphere followed by argon-gas quenching to 300 K. The average grain size as annealed was approximately $3 \times 10^{-5}$ m. Sample thickness ranged from 1 to $1{\cdot}2 \times 10^{-3}$ m. Sample length and width were each $2 \times 10^{-2}$ m. Before use, the specimens were electropolished with a Bollman solution†.

Cathodic hydrogen charging was done by the method of Boniszewski and Smith (1963). This procedure does not produce nickel hydride on the surface of the sample. The charging conditions are :

(*a*) Bath : 1N $H_2SO_4$ solution.
(*b*) Charging temperature : 364–367 K.
(*c*) Current density : 125–500 A/m$^2$.
(*d*) Anode : platinum foil.

Since the P/W Doppler lineshape factor is an indirect index for the extent of hydrogen embrittlement, microhardness measurements were made to supplement the Doppler broadening results. By using a diamond pyramid indentor

† Bollman solution : $H_3PO_4$(860 cm$^3$) + $CrO_3$(100 g) + $H_2SO_4$(51 cm$^3$).

and a 1 kg load, dislocations were introduced around the 1 kg impression. Microhardness measurements then were made along two orthogonal directions, (1) and (2) in fig. 2. As soon as the microhardness measurements were made, the indented sample was cathodically charged with hydrogen for 1 hour. The microhardness distribution was then measured using a 25 g load along two other orthogonal paths, marked (3) and (4) in fig. 2. In order to see if there was any significant thermal effect on microhardness during cathodic charging at 364–367 K, a similarly indented sample was held for 1 hour in a 365 K water bath to simulate the charging bath. The microhardness was then measured as above.

Fig. 2

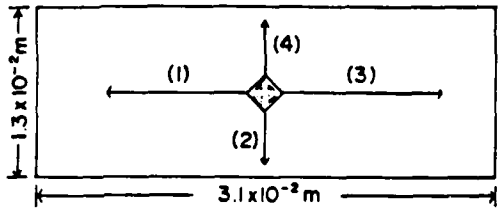


Schematic diagram of microhardness measurement directions.

## § 3. Results

The Doppler lineshape factor of annealed samples strained in tension increased with increasing strain† as shown in fig. 3. Doppler P/W measurements for various times of hydrogen charging for cold-worked samples are shown

Fig. 3

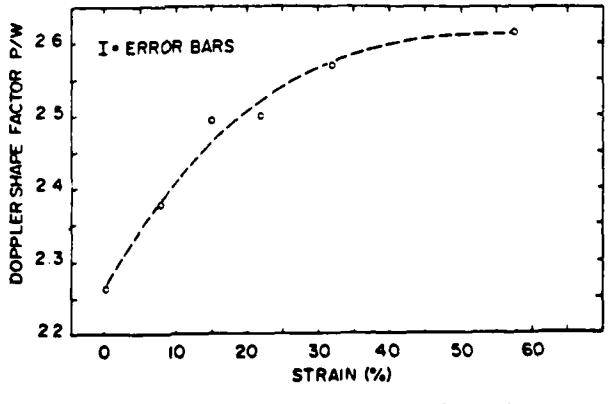


Doppler shape factor versus tensile strain.

† Engineering strain.

in figs. 4, 5 and 6. The P/W ratio increases with increasing charging time. This increase takes the form of two successive steps in figs. 4 and 5 and a single step in fig. 6 which is for very slightly deformed material. In order to examine the reproducibility of these phenomena, a second 70% cold-rolled sample was investigated under exactly the same experimental conditions. The data are marked as Sample No. 2 on fig. 4 and show good agreement with Sample No. 1.

Fig. 4

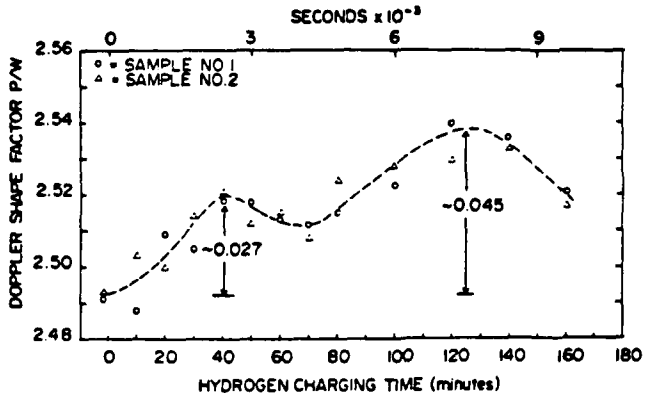


Hydrogen charging of 70% cold-rolled nickel. ○ = Sample No. 1 ; △ = Sample No. 2 ; current density = 200 A/m².

Fig. 5

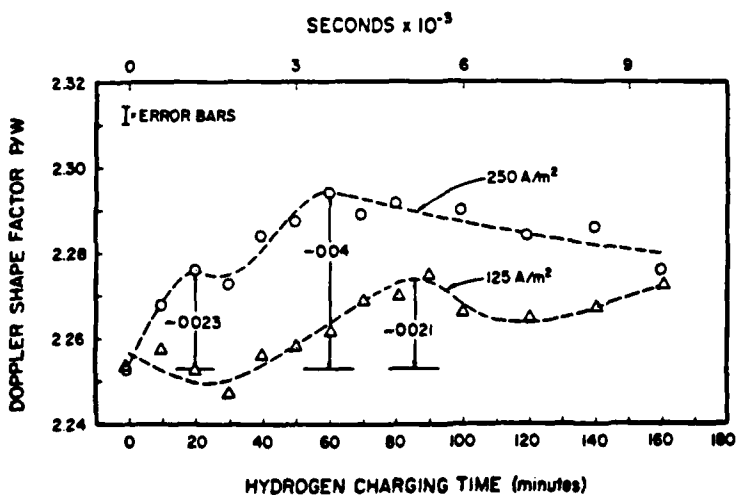


Hydrogen charging of 10·7% strained nickel at current densities of 250 and 125 A/m².

Fig. 6

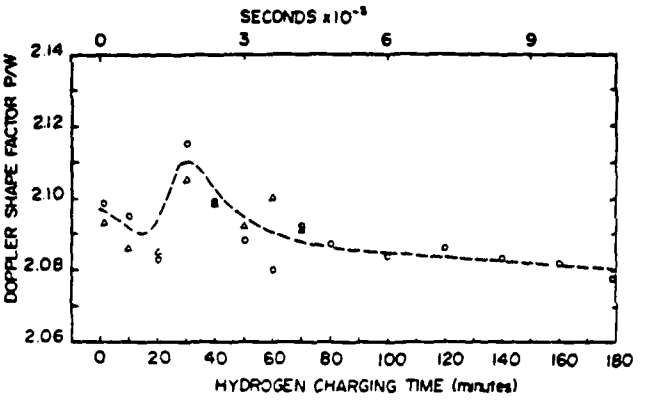


Hydrogen charging of 0·87% strained nickel. ○ = Sample No. 3 ; △ = Sample No. 4 ; current density = 250 A/m².

The effect of the magnitude of the charging current density was investigated by charging identically strained samples at current densities of 250 and 125 A/m² as shown in fig. 5. The data for a current density of 250 A/m² first levels off at P/W = 2·275 which is the same as the highest P/W level of the 125 A/m² data of fig. 5. In addition, an annealed sample was charged repeatedly up to 3 hours with no significant change of Doppler shape factor. The more severe the prior plastic strain, the larger the increment in Doppler lineshape factor caused by hydrogen charging.

A linear recovery effect was noted in a 70% cold-rolled sample held in a 365 K water bath. The P/W value dropped from 2·50 to 2·47 in 250 min.

Fig. 7

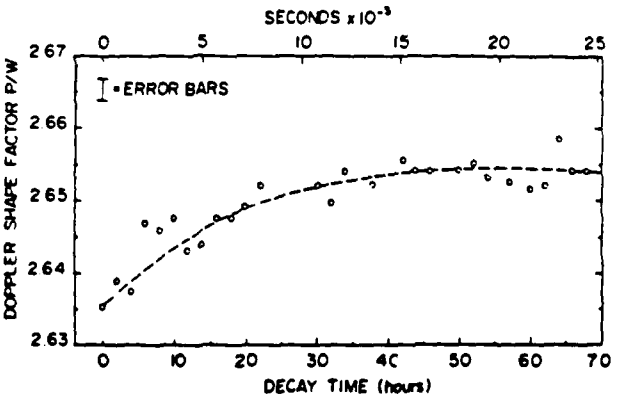


Decay of hydrogen charged 70% cold rolled nickel. Current density = 250 A/m² ; charging time = 3 hours.

Another 70% cold-rolled specimen was cathodically charged for 3 hours and then measured as a function of time at 300 K. Figure 7 shows an interesting increase in P/W during this period. A saturation limit of P/W was reached after approximately 40 hours.

Microhardness measurements from all samples were related to the distance from the large (1 kg) impression by computer-aided curve fitting. The following two functions resulted.

Samples Nos. 9 and 10 :

(1) after hydrogen charging : $H_1 = 125{\cdot}54 + 0{\cdot}2273a^{-1} + 0{\cdot}00126a^{-2}$ (standard deviation = 3·36) ;

(2) before hydrogen charging : $H_2 = 94{\cdot}60 + 0{\cdot}3535a^{-1} - 0{\cdot}00242a^{-2}$ (standard deviation = 1·95) ;

where $a$ is the distance from the large indentation in $10^{-3}$ m, and $H$ is the Vickers microhardness (25 g).

Fig. 8

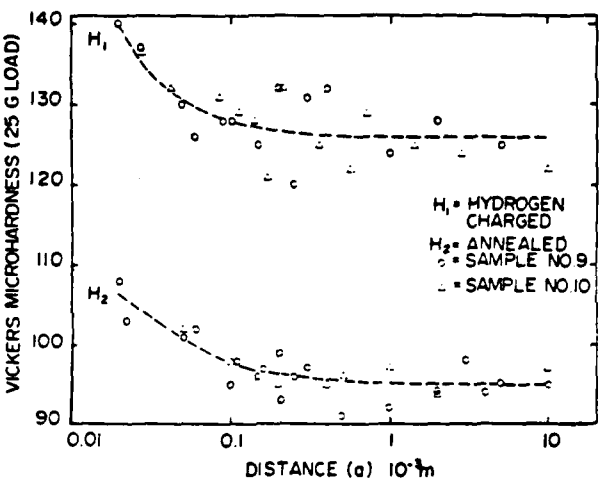


Vickers microhardness versus distance from main (1000 g) indentation for : $H_1$ = Annealed and indented ; $H_2$ = Annealed, indented and charged at 500 A/m².

The data showing the effect of hydrogen charging versus distance from the large impression are plotted as $H_1$ in fig. 8. The effect of a 1-hour thermal treatment at 365 K was essentially the same as shown by the data distribution marked $H_2$ in fig. 8 which is actually for the 973 K annealed condition.

From both microhardness and Doppler broadening measurements, a consistent trend is found in which hydrogen causes a hardening effect proportional to the original degree of cold work. This hardening effect is over and above any recovery of the degree of cold work which results from annealing due to the heat of the charging bath.

## § 4. Discussion

The increase of the Doppler P/W lineshape factor in fig. 3 is frequently observed and interpreted as an increase in the number of positron traps, i.e. an increase in defect density. In the present work an increase of the P/W lineshape factor also was generally found upon the initial hydrogen charging of cold worked nickel as in figs. 4, 5 and 6. The best interpretation of this increase is in terms of an increase in defect density during hydrogen charging. Proton trapping at dislocations of itself would have to produce a decrease of P/W, since the attractive negative potential of vacancies or dislocations for positrons would be reduced (screening) by the presence of protons at such defects.

Two possibilities are suggested for the increase in defect (mostly dislocation) density in nickel upon hydrogen charging :

(1) Protons and/or hydrogen atoms accumulate at existing discontinuities such as inclusions, grain boundaries or voids. According to Troiano (1974) inclusions *are* voids in the sense of dissolved hydrogen in the crystalline lattice. Cathodic hydrogen charging is well known to occur under external surface fugacities equivalent to virtual hydrogen pressures of thousands of atmospheres. Thus, high supersaturations of internal hydrogen are created (Troiano 1974) which in turn can result in high molecular hydrogen pressure in voids and stress in the solid near the void. Stress around a pressurized void can generate dislocations (DiMartini and Byrne 1964, Wampler *et al.* 1976) and a high dissolved localized hydrogen concentration (Troiano 1974, Gerberich, Garry and Lessar 1975). Such newly generated dislocations will be less likely to become saturated with protons than will those dislocations initially present and, therefore, they should be able to give rise to an increase in the P/W lineshape factor.

(2) As a localized high concentration of hydrogen segregates at a defect, nickel hydride may be formed. The misfit caused by the 5·5% larger lattice parameter of the hydride (Wollan, Cable and Koehler 1963) would be enough to produce plastic strain and hence dislocations. The hydride is unstable and will decompose to Ni and hydrogen gas which is highly immobile in Ni. Wollan *et al.* (1963) found the hydride to be completely decomposed in cathodically charged nickel within 6 to 8 hours.

Maximum values in the Doppler P/W lineshape factor are seen in figs. 4, 5 and 6. The decrease in P/W factor following a maximum can be explained by the proton screening of the defects as mentioned in § 1. Usually the tensile side of the edge dislocation and the vacancy are regarded as defects with effective negative charge. A proton trapped in such a region tends to reduce the positron trapping ability of the region ; hence P/W decreases in the presence of trapped protons. The same phenomenon was observed with positron-lifetime measurements by Alex *et al.* (1975) in that a decrease of positron lifetime was observed after reaching the saturation lifetime upon hydrogen charging. However, in the present work, none of the P/W maxima reached a saturation value in nickel. Therefore, it is expected that upon further charging, following a minimum in P/W, the Doppler lineshape factor should rise again. This was observed as shown in figs. 4 and 5. Microhardness increases caused by hydrogen charging are only slightly larger in the region with an initially higher defect density, i.e. closer to the 1000 g central indentation of fig. 2

than in regions far from the indentation. This may be seen by comparing the differences between data sets $H_1$ and $H_2$ at the left-hand and right-hand sides of fig. 8.

Cathodic charging of the annealed Ni produced no change in P/W shape factor, yet the microhardness of the annealed Ni was increased by charging, as is shown by the right end of curve $H_1$ in fig. 8, i.e. the charging effect far from the large indentation. This is interpreted as meaning that, in terms of P/W ratio, the charging of annealed material resulted in an exact balancing of defect generation and the proton screening of those defects from the positrons, yet the existence of the defects is sufficient to affect the microhardness. An additional source of the microhardness increase in any region, and one which would not respond to positron measurements, is that of solid-solution hardening of the lattice due to hydrogen atoms in interstitial positions. The microhardness of this material was unchanged after 50 days at ambient temperature. This indicates that the dislocation density remained constant during this time.

Bauer and Schmidbauer (1961) and Oriani (1967) found that hydrogen enters the lattice as a proton which has given up its electron to the conduction band of the metal. Given the existence of protons in Ni, the screening effect of a proton (on a defect) becomes more acceptable. The upward trend of P/W values in fig. 7 for charged Ni left at ambient temperature for 70 hours may have several causes. One is that some protons may diffuse out of the sample by dislocation short-cut diffusion, unscreening some dislocations and thus raising the value of P/W. Another is that protons de-trapped from dislocations or delivered by dislocation diffusion to inclusions or certain grain boundary locations, may combine to form $H_2$ and generate new dislocations by exerting pressure. Louthan (1974) has estimated pressures of tens of thousands of atmospheres at such locations. The new unscreened dislocations would raise the P/W ratio. Optical microscopy of polished and unetched specimens which had been charged revealed considerable grain-boundary delineation due to $H_2$ segregation. Similarly nickel hydride, as it decomposes, could contribute $H_2$ to a pressure centre at room temperature. This latter cause is less certain because as the hydride decomposed one also would lose the 5·5% lattice disregistry which would probably cause P/W to decrease rather than increase.

The lower curve in fig. 5 and the curve in fig. 6 each show slight initial decreases in P/W ratio. This is attributed to the probable greater ease of proton screening of existing defects relative to the process of defect formation by either of the two mechanisms suggested earlier. Given more charging time the hydrogen concentration increases so as to allow defect generation to become predominant over defect screening by protons and recovery effects.

Both curves in fig. 5 indicate a structural dependence of the Doppler lineshape factor value at the first step in each plot. That is, for the same amount of prior cold work, the value of P/W reached at the first step is the same for both current densities. The slightly lower P/W value at the first step in fig. 5 for 125 A/m² may be accounted for by the longer time for recovery during charging at the lower current density (four times longer at half the current density).

The cyclic character of figs. 4, 5 and 6 may also be related to depth considerations. Based on the space distribution of thermalized positrons (Brandt 1974), the hydrogen embrittlement near the entrance surface must contribute

more to the change of Doppler shape factor than does the embrittlement occurring deeper inside the sample. In the initial period of charging, the increase of Doppler shape factor results from new defects produced by the segregated hydrogen (either hydrogen gas or hydride) in the region near the positron entrance surface. At the same time, protons are continuously trapped by the newly formed as well as the old defects. When the proton screening effect can overwhelm the effect of positron trapping at new defects, a decrease of Doppler shape factor results. This is suggested as the sequence of events up to the time a first minimum appears. Upon further charging, more new defects may be generated from internal pressure centres or hydrides in some deeper region as well as in the region near the surface. Then another cycle of the variation of Doppler shape factor starts. In the second cycle, the defect production rate decreases in the near surface region. Since the positron probe is less sensitive in the deeper region (only one positron energy was used throughout), a longer time is needed to reach the second maximum. Furthermore, one sees a smaller increase in P/W shape factor from the first to the second maximum than the increase from the initial point to the first maximum, as would be expected.

## § 5. Conclusions

Hydrogen charged into nickel creates defects (dislocations) which may be effectively detected with the positron Doppler broadening technique.

Pre-existing defects such as dislocations and surfaces such as grain boundaries and inclusion-matrix interfaces may serve as proton trapping sites. The latter two types of site probably also serve as locations for the formation of molecular hydrogen pressure centres.

In hydrogen-charged nickel the detrapping of protons from dislocations occurs as a relaxation process with time at ambient temperature. This results in a decrease in positron Doppler broadening (i.e. an increase in P/W shape factor) to a stable value.

Cyclic behaviour in the P/W Doppler shape factor during continued hydrogen charging is indicative of the following sequence of events: defect generation, proton screening of some defects from positrons, generation of new defects, etc.

## Acknowledgments

The authors are grateful for the support of the U.S. Department of Energy and the Air Force Office of Scientific Research in this work. The helpful comments of Dr. K. G. Lynn were much appreciated.

## References

Alex, F., Hadnagy, T. D., Lynn, K. G., and Byrne, J. G., 1975, *International Conference on Effect of Hydrogen on Behavior of Materials* (The Metallurgical Society of AIME), p. 642.

Bauer, H. J., and Schmidbauer, E., 1961, *Z. Phys.*, **164**, 367.

Boniszewski, T., and Smith, G. C., 1963, *Acta metall.*, **11**, 165.

Brandt, W., 1974, *Appl. Phys.*, **5**, 1.

DiMartini, R. G., and Byrne, J. G., 1964, *J. Phys. Chem. Solids*, **25**, 147.

GERBERICH, W. W., GARRY, J., and LESSAR, J. F., 1975, *International Conference on Effect of Hydrogen on Behavior of Materials* (The Metallurgical Society of AIME), p. 70.

JOHNSON, M. L., 1977, M.S. Thesis, University of Utah.

JOHNSON, M. L., SATERLIE, S., and BYRNE, J. G., 1978, *Metall. Trans.*, **9A**, 841.

LICHTENBERGER, P. C., 1974, Ph.D. Thesis, University of Waterloo.

LOUTHAN, M. R., 1974, *Hydrogen in Metals*, edited by I. M. Berenstein and A. W. Thompson (Metals Park, Ohio : American Society for Metals), p. 53.

ORIANI, R. A., 1967, *Proceedings of the Symposium on Stress Corrosion Cracking*, Houston (N.A.C.E.), p. 37.

SEEGER, A., 1974, *Appl. Phys.*, **4**, 183.

TROIANO, A. R., 1974, *Hydrogen in Metals*, edited by I. M. Berenstein and A. W. Thompson (Metals Park, Ohio : American Society for Metals), p. 53.

WAMPLER, W. R., SCHOBER, T., and LENGELER, B., 1976, *Phil. Mag.*, **34**, 129.

WEST, R. N., 1973, *Adv. Phys.*, **22**, 263.

WOLLAN, E. O., CABLE, J. W., and KOEHLER, W. C., 1963, *J. Phys. Chem. Solids*, **24**, 1141.

PHILOSOPHICAL MAGAZINE A, 1979, VOL. 40, NO. 1, 143

# ERRATUM

*A study of hydrogen charging of nickel by positron Doppler broadening.* By P.-W. KAO, R. W. URE, JR., and J. G. BYRNE, 1979, *Phil. Mag.* A, **39**, 517.

The caption below fig. 8 of this paper contains an error which the authors now correct. Although the curves are labelled correctly in the figure, they are wrongly identified in the caption, which should read :

Vickers microhardness versus distance from main (1000 g) indentation for : $H_1$ = Annealed, indented and charged at 500 A/m$^2$ ; $H_2$ = Annealed and indented.


FILMED
0-8